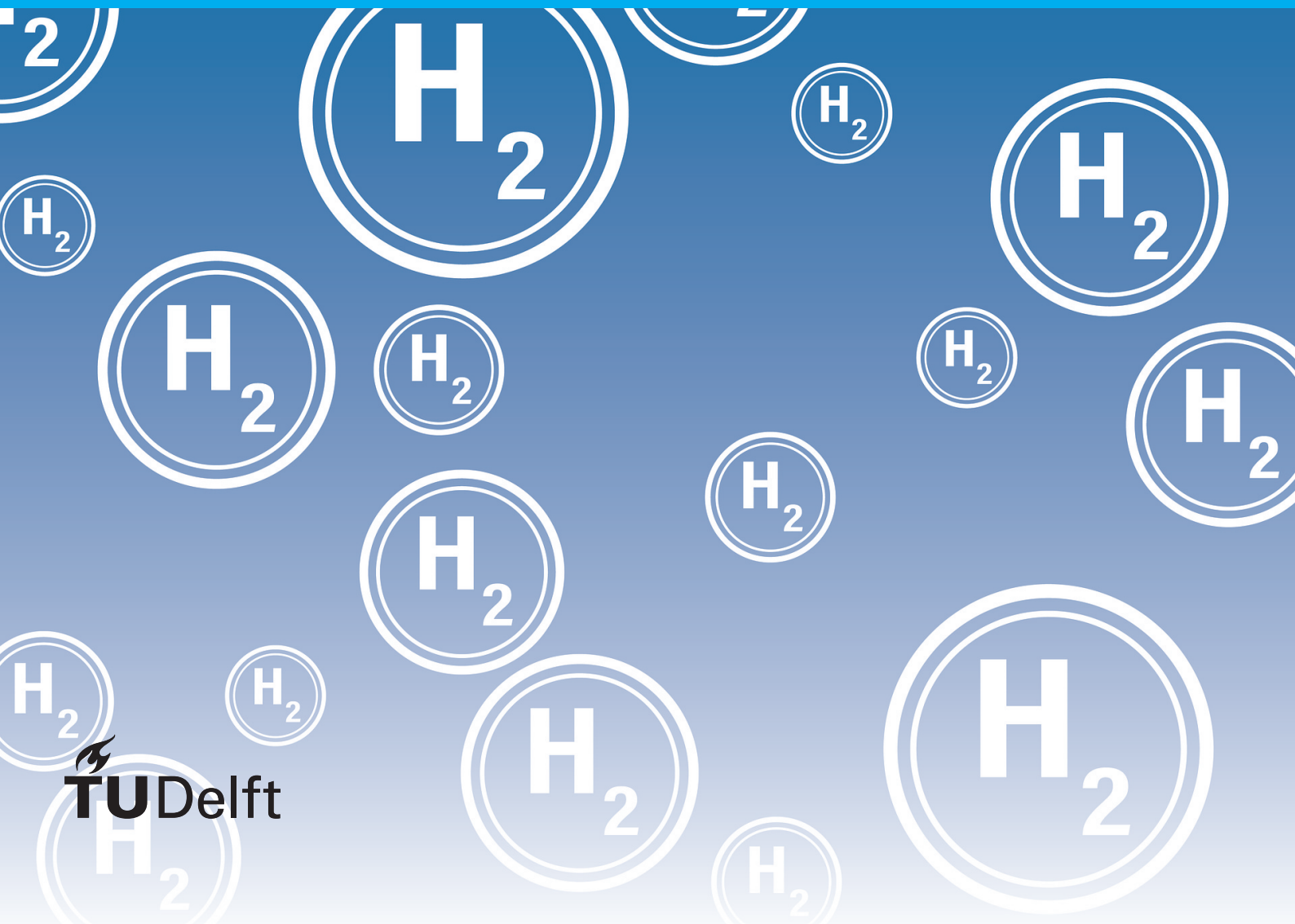


Economic analysis of a renewable hydrogen supply chain between Northern Africa and the European Union

An optimization-based study towards the economic feasibility of renewable hydrogen based on a case study using currently available technologies

J.M. Janssen



Economic analysis of a renewable hydrogen supply chain between Northern Africa and the European Union

An optimization-based study towards the economic feasibility of renewable hydrogen based on a case study using currently available technologies

by

J.M. Janssen

07-02-2023

to obtain the degree of Master of Science
at the Delft University of Technology,

to be defended publicly on Tuesday February 14, 2023 at 10:00 AM.

Student number: 4629418
Project duration: December 2021 - Februari 2023
Thesis committee: Prof. dr. ir. Z. Lukszo, TU Delft,
Dr. ir. M. d. M. Pérez-Fortes, TU Delft
Dr. A. Schweidtmann, TU Delft
Dr. N. Li, TU Delft

Summary

The European Union has set out to become carbon neutral by 2050. To reach this goal, the fossil-fuel-dominated energy system must be transformed into a low-carbon renewable-based energy system. One method proposed to reduce fossil-fuel dependence is to establish a renewable hydrogen supply chain between Africa and the European Union. This work provides a model framework that enables an economic analysis of a renewable hydrogen supply chain between northern Africa and the EU. The aim of this work is to gain a better understanding of large-scale intercontinental renewable hydrogen production by investigating the factors that impact the economic performance of this system.

A mixed-integer linear programming model that describes the supply chain is built, and modeled in Python and a case study defining the overall energy system under consideration and applied to this model. The system must provide 780 TWh of hydrogen demand for the EU in 2050. Hydrogen is produced by water electrolysis, using renewable electricity from solar photovoltaics. The water required for electrolysis is supplied through reverse osmosis of seawater. Seasonal storage of hydrogen is enabled through the inclusion of hydrogen storage in salt caverns.

The resulting annual costs of operating the supply chain are 36.55 B\$, corresponding to a levelized cost of hydrogen of 1.56 \$kg⁻¹. The main contributors to the cost of the supply chain are solar photovoltaics (50%), alkaline electrolysis (22%), and transportation (26%). Through a sensitivity analysis on price uncertainty, it is found that the system is most sensitive to photovoltaics prices (59%), electrolysis prices (21%), and hydrogen pipeline prices (18%). A sensitivity analysis of the interest rate on capital investment points towards a significant impact of the interest rate on the total annual cost.

The findings of the model and applied case study in this work are then compared to projected costs in other works. From this analysis, it is found that hydrogen production using electrolysis will be cheaper than fossil-based low-carbon hydrogen production alternatives in the form of steam methane reforming or coal gasification with carbon capture technology. Predictions of the selected works regarding electrolysis-based hydrogen production using renewable electricity show an expected LCOH of between 1.66 - 2.39 \$kg⁻¹.

This work indicates that a renewable hydrogen supply chain between Morocco and the EU in 2050 is both technically and economically feasible, able to compete with alternative hydrogen production methods, and able to supply 35% of the projected hydrogen demand. Moreover, this work developed a general hydrogen supply-chain model that allows for the implementation of additional features as well as the analysis of different case studies through the adjustment of case-specific parameters.

Preface

This thesis marks the end of six and a half years of studying at the TU Delft. Throughout this time, I have learned many useful skills, met a lot of great people, and worked on projects close to my heart. This research in particular gave me the opportunity to work on a project I was already interested in and allowed me to work out in-depth the questions I had. I would like to thank Dingena Schott, Mar Pérez-Fortes, Artur Schweidtmann, and John Posada Duque for giving me this opportunity.

As my daily supervisor, I would like to thank you Mar for all the guidance on the project, the countless hours of supervision, for always believing in me, and for introducing me to new people to help me. I was introduced to Josephine Vos and Thijmen Wiltink, who helped me shape the project at the start and were there to answer my questions. Next, I would like to thank Artur for his feedback on the project, his kind words and positivity, and the introduction to his research group, which in times of Covid, gave me some well-needed contact with other students. Furthermore, I want to thank Zofia Lukszo for looking after both my project as well as my personal well-being. Zofia helped me understand my project on a level of detail I believe I was not reaching on my own. Mar and Zofia also introduced me to Na Li, who helped me shape and structure the report, for which I am truly grateful. Finally, I want to thank Rianne Janssen, my sister, for providing me with loads of feedback to work with and helping me clearly put my ideas onto paper. I am proud of the work I have delivered, and without all of you, it would have been impossible.

J.M. Janssen
Delft,

Contents

Summary	iii
Preface	v
1 Introduction	3
1.1 Problem statement	6
1.2 Knowledge gaps	7
1.3 Research questions	8
1.4 Thesis scope and goals	9
1.5 Research approach	9
1.6 Thesis outline	10
2 System design	11
2.1 System description	11
2.2 Technology selection	13
2.2.1 Electricity generation	14
2.2.2 Water purification	15
2.2.3 Electrolysis	17
2.2.4 Storage	20
3 Approach	23
3.1 Model overview	23
3.2 Optimization model	26
3.2.1 Objective function	27
3.2.2 Constraints	29
3.3 Performance indicators	32
4 Case study	35
4.1 Overview	35
4.2 Input data and assumptions	35
4.2.1 Production technologies	37
4.2.2 Transportation	39
4.2.3 Storage	39
4.3 Cost parameters	40
4.4 Assumptions	40
5 Results analysis	43
5.1 System sizing and transport strategy	43
5.2 System operations	44
5.3 System costs	46

5.4	Sensitivity analysis	49
5.4.1	Technology costs	49
5.4.2	Interest rate	49
5.4.3	Initial conditions	50
5.5	Discussion of results	51
5.5.1	Cost comparison to alternative supply chains	51
6	Discussion and recommendations	55
6.1	Main findings	55
6.2	Model limitations	56
6.3	Case study limitations	57
6.4	Recommendations	58
7	Conclusion	61

List of Figures

1.1	Photovoltaic power potential across Africa and the Middle East, from [11]	4
1.2	Average wind speed across Africa and the Middle East, from [12]	5
2.1	Schematic representation of the hydrogen supply chain under consideration.	12
2.2	System layout of the supply chain model. Echelons are colored yellow (solar plant), blue (water treatment), orange (electrolysis), green (storage), and red (demand).	13
2.3	Illustration of the working principle of a solar cell based on a p-n junction under the presence of an external photon source. Retrieved from [42].	14
2.4	Thermodynamics of water electrolysis. Retrieved from [52]	18
2.5	Schematic representation of an alkaline electrolyzer. Retrieved from [53]	19
2.6	Schematic representation of a PEM electrolyzer. Retrieved from [53]	19
2.7	Pressure and temperature dependence on the density of compressed hydrogen gas. Retrieved from [61]	21
4.1	Normalised electricity demand for the European Union based on monthly electricity consumption. Original data retrieved from [72]	37
4.2	Scatterplot of the amount of peak solar hours equivalence of solar irradiation at the location of the power plant for every month in one year. Original data retrieved from [73]	38
4.3	Schematic representation of the workflow of obtaining the input parameters that are used in the optimization model.	41
5.1	System layout of the supply chain model. Echelons presented are the solar plant (yellow), SWRO plant (blue), electrolysis (orange), hydrogen storage (green) and hydrogen demand (red). The lines between echelons indicate utilized transport connections. Transport connections utilized are for electricity (yellow, water (blue) and green (hydrogen)).	45
5.2	Sankey diagram of energy flows of the optimized supply chain.	46
5.3	Capacity factors of the electricity generation, electrolysis, and water treatment plants throughout the year.	47
5.4	Overview of monthly hydrogen demand, hydrogen production, storage amount, and storage in- and outflow.	47
5.5	Cost breakdown of the LCOH of hydrogen in the proposed supply chain and case study	48
5.6	Tornado plot of the performed sensitivity analysis. The plot shows the cost ranges for the overall system as a result of price uncertainty for the various technologies.	50
5.7	Sensitivity of the model to the interest rate. Interest rate ranges from 0% to 10%. The general model assumes a value of 7%. The sensitivity is shown to both the TAC (red) and LCOH (blue).	51

List of Tables

2.1	Thermodynamic properties for reaction 2.1	17
2.2	Summary of parameter comparison between AEL, PEM, and SOEL ([57–59]).	20
4.1	Echelon locations and parameters adopted in the model	36
4.2	Irradiation and solar PV capacity factor for every month as used in the case study. Original data retrieved from [73]	39
4.3	Overview of future cost estimations for PV systems	39
4.4	Overview of future cost estimations for AEL systems	40
4.5	Assumed costs for transportation infrastructure.	40
4.6	Distance (km) between echelon locations	41
4.7	Overview of economic parameters for various technologies adopted for the case study	41
5.1	Size and land use for the PV, electrolyzer and SWRO plants.	44
5.2	Cost breakdown comparison of LCOH	49
5.3	Effect of initial storage on the optimal size of the PV, electrolyzer and water treatment plants.	51
5.4	Results of sensitivity to the starting month of the model. Inf indicates the starting month results in an infeasible problem	52
5.5	Cost comparison table of various low carbon hydrogen production methods. The compared technologies are Steam Methane Reforming (SMR), Coal Gassification (CG) and electrolysis. For GC and SMR, the cost of CCS is included.	52

Nomenclature

Acronyms

AUC	African Union Commission
CCS	Carbon capture and storage
CF	Capacity Factor
CF	Capacity factor
CG	Coal gasification
EAC	Equivalent Annual Cost
EU	European Union
HSCND	Hydrogen supply chain network design
HVAC	High voltage alternating current
LCOH	Levelised cost of hydrogen
LHV	Lower heating value
MSF	Multi-stage flash distillation
OPEX	Operational expenditures
PV	Photovoltaics
RO	Reverse osmosis
SMR	Steam methane reforming
SWRO	Seawater Reverse Osmosis
TAC	Total Annual Cost
VCD	Vapor compression distillation

1

Introduction

Ever since the start of the industrial revolution in the 18th century, energy has been produced using fossil fuels. This has led to a worldwide energy system, dominated by and designed for fossil fuels. Nowadays, it is widely accepted that using fossil fuels to produce energy is unsustainable, as the pollution resulting from the use of fossil fuels is shown to have severe economic, environmental and sociological consequences [1].

Concerns about the adverse effects of fossil fuel use and resulting climate change were carefully expressed already in the 19th century and substantiated in the early 20th century. The first internationally recognized conference on climate change was the 1979 World Climate Conference in Geneva [2]. In the years after this first conference, more attention was drawn to the issue of climate change. As a result, climate change science was started and world leaders started to recognize the possible impact of man-made climate change. The first internationally accepted treaty on combatting man-made climate change was the Kyoto protocol signed in 1997. However, ratification of the Kyoto protocol took until 2005, due to the withdrawal of the United States [2]. The next big leap was the 2015 Paris agreement that set the goal for member states to reduce carbon emissions as soon as possible and keep global warming well below 2°C [3].

In order for The European Union (EU) to reach its climate goals, it has set a target for 2050 to become carbon neutral as part of the European Green Deal [4]. As part of the Green Deal, the European Commission stresses the need for the supply of "clean, affordable and secure energy" as well as "mobilising industry for a clean and circular economy" [4]. More recently, the EU has presented the REPowerEU plan, which aims to reduce energy dependence through energy savings, diversifying the energy supply, and accelerating the energy transition [5]. A drastic overhaul of the current energy system is required in order to meet the objectives of the REPowerEU plan.

Changing the energy system of a continent within just over 25 years will be a major challenge to overcome. However, this is not the only major challenge for the EU on the path to carbon neutrality. Currently, the EU is dependent on other countries for over 60% of its total energy supply [6]. This has become very clear only recently, when energy imports dropped as a result of the conflict between Russia and Ukraine, with soaring energy prices in the EU as a result [7]. Even if the EU would become

less dependent on imported energy, it is expected that the EU will not be able to cover its full energy demand using renewable energy sources relying on domestically produced energy [8]. Therefore, an energy supply chain providing the EU with additional renewable energy must be secured for the EU to reach its climate goals. In order to realize such a supply chain, it is expected that cooperating in a mutually beneficial relation with neighboring regions, for example, Northern Africa or Western Asia will be required.

Due to its proximity to the EU and high renewable energy potential, as shown in Figures 1.1 and 1.2 [8, 9], Northern Africa makes a suitable candidate for a mutually beneficial cooperation. Establishing a renewable energy supply chain between Northern Africa and the EU would not only provide the EU with renewable energy, but it could also present social and economic development opportunities for the Northern African region [10]. These development opportunities seem to be aligned with the visions developed by the African Union Commission (AUC).

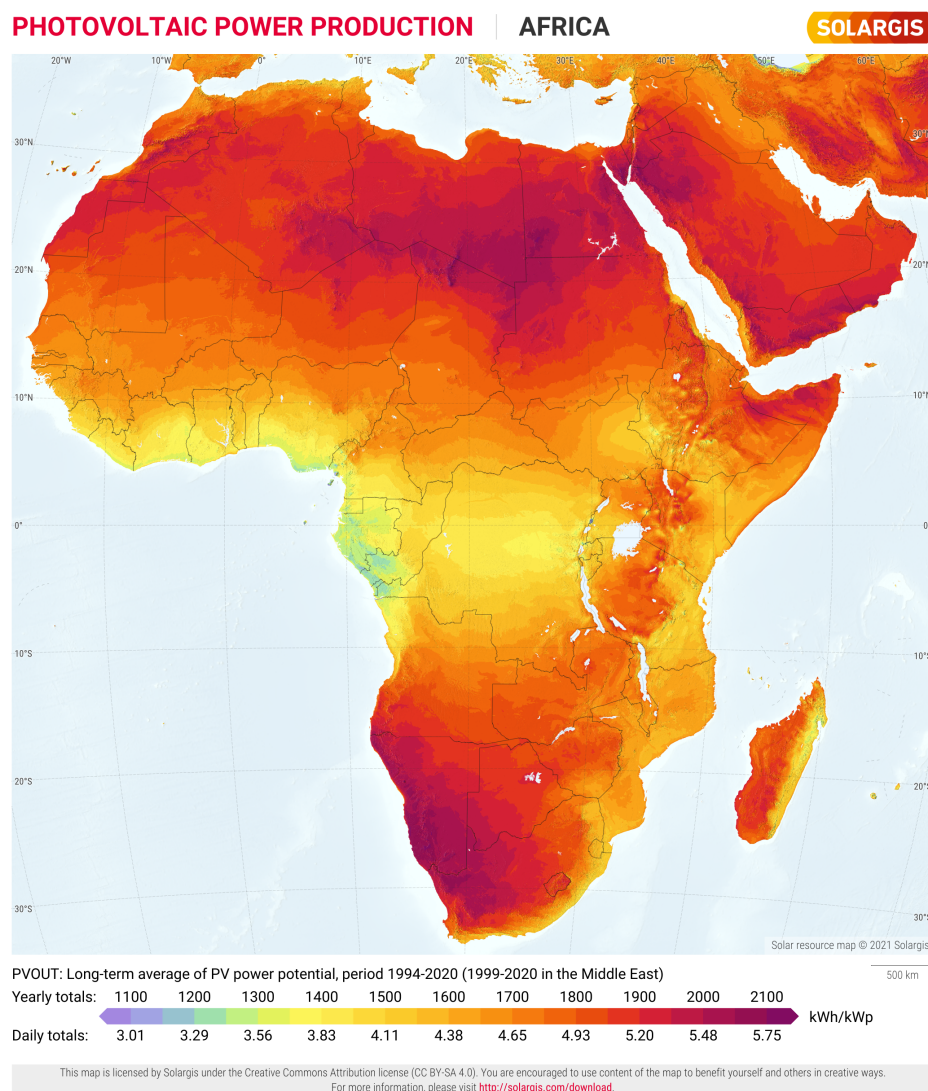


Figure 1.1: Photovoltaic power potential across Africa and the Middle East, from [11]

In Agenda 2063, goals are set out to transform the African continent into a prosperous and peaceful continent. In this vision, the AUC wants to phase out poverty by a social and economic transformation

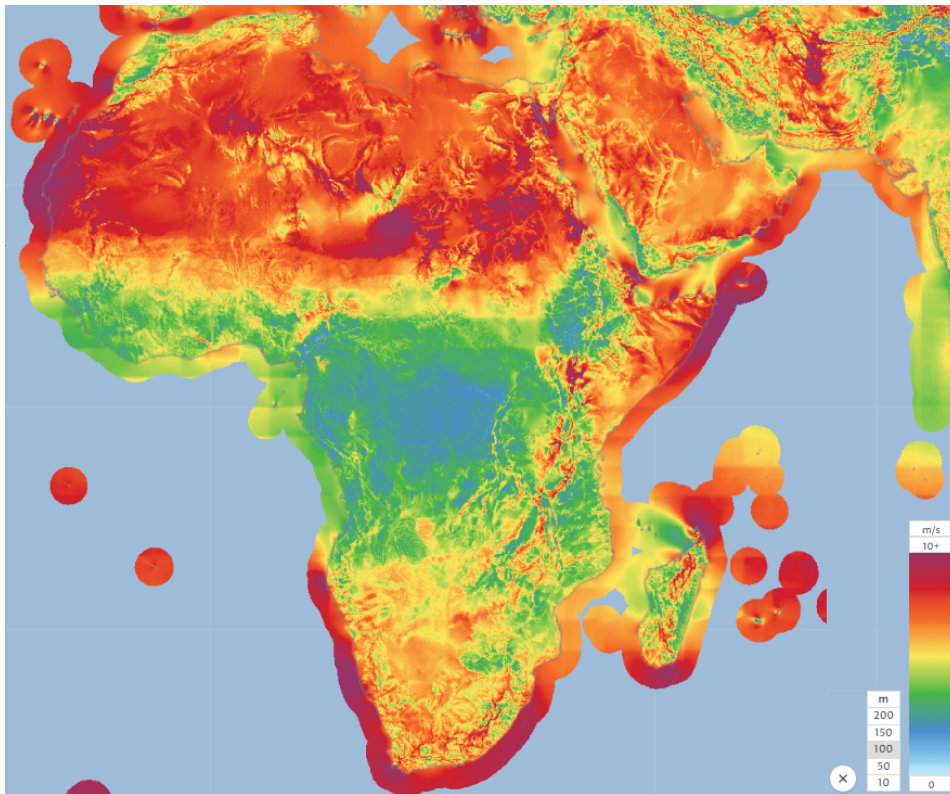


Figure 1.2: Average wind speed across Africa and the Middle East, from [12]

of African society [13]. To achieve this transformation the AUC proposes to kickstart industrialization and promote investments in science, technology, and innovation while taking responsibility to mitigate climate change, under sustainable use of resources. To reach the transformation, the AUC is looking to finance development in transport, energy, and digital infrastructure by seeking mutually beneficial relations with parties outside of the African continent. The future vision of the AUC shows that there is room for mutually beneficial projects regarding energy production and transportation, and a willingness from both the EU and AUC to establish such projects. However, envisaged projects should not conflict with other long-term goals put out by the AUC, such as the improvement of basic living conditions for African citizens, including access to food, water, and energy.

It is clear that both the EU and AUC are willing to participate in a mutually beneficial relationship regarding renewable energy production. It is therefore of interest to investigate how such an intercontinental supply chain would be established. In general, an intercontinental renewable energy supply chain between Northern Africa and the EU should fulfill at least three requirements. First, this supply chain must produce renewable energy. Second, it must be able to transport this energy between continents over long distances. Finally, it must be able to store this energy on daily, weekly, and monthly timescales to accommodate both variances in supply and demand. It is therefore proposed to use hydrogen as an energy vector for such a supply chain, as hydrogen is easy to transport and store [4, 8, 10, 14].

From the perspective of a supply chain, utilizing hydrogen as an energy vector has clear benefits compared to electricity regarding transport and storage. Additionally, from an environmental perspective, using hydrogen as an energy carrier would enable sectors outside of the energy sector, for example, industry, to reduce carbon emissions. Hydrogen is a mass-produced commodity, amounting to approximately 4% of global final energy consumption, of which 95% is produced using fossil fuels [10].

Therefore, producing renewable hydrogen would already enable the decarbonization of current hydrogen uses, for example as feedstock for ammonia synthesis for fertilizer production. Other large-scale industries, for example, steel and cement production, can also utilize renewable hydrogen to decarbonize the production processes as direct feedstock or fuel for industrial heat respectively [14].

Although renewable hydrogen production may reduce carbon emissions in the energy industry and energy-intensive sectors, lots of water is required for its production. Large-scale renewable hydrogen production in Northern Africa may therefore cause conflict with regional water availability. Water scarcity is a worldwide phenomenon, described as the lack of water safe for consumption. Water scarcity is often divided into physical water scarcity, where water is not present in sufficient quantities, and economic water scarcity, where the cost of water may be too high for utilization by the general public. According to the United Nations, the highest water stress worldwide, related to physical water scarcity, is in Northern Africa [15].

The risk of water scarcity is amplified by a multitude of influencing factors, most prominently being climate change and population growth. The effects of climate change and global warming are expected to be much worse in Africa compared to the global average. Increasing temperatures will result in water loss by the drying-out of water basins [16]. Moreover, global warming is responsible for shifting rainfall precipitation patterns, from which Northern Africa, already one of the only African regions with physical water scarcity, is impacted the most [16].

As populations grow, food and water consumption also increase. This is particularly relevant to the African continent, as population growth in Africa is higher than in any other continent. It is expected that the African population will double by 2050. Related to population growth is the phenomenon of urbanization. Specifically, in low-income countries, population growth and urbanization result in unplanned settlements near urban centers [17]. Often, these unplanned settlements do not have access to basic services such as clean drinking water, drainage, and electricity, adding to the problem of water scarcity [17].

When designing a hydrogen supply chain starting in Northern Africa, measures can be taken in order to reduce the risk of water scarcity for the regional population. Alternative water sources that do not directly compete with existing water consumption can be used in order to reduce the dependency on water availability. For example, the use of seawater as an alternative to freshwater as feedstock for water electrolysis can reduce the risk of water scarcity.

1.1. Problem statement

As of December 2019, the EU has pledged to become carbon neutral by 2050 through the European Green Deal [4]. For this to be achieved, the current energy system based on fossil fuels must be replaced with less carbon-intensive alternatives. This may be done in part by locally producing energy from renewable sources such as the sun and wind. However, it is expected that demand cannot be met with domestic supply. Therefore, it may be interesting to explore the possibility of importing energy from outside of the EU, with Northern Africa as a promising candidate.

Africa has a large renewable energy potential. Northern Africa in particular has an abundance of renewable energy potential due to high solar irradiation and wind speeds, enabling the production of renewable electricity using renewable energy technologies. On top of this, Northern Africa is in proximity to southern Europe and an energy infrastructure between the two regions is already present.

Therefore, Northern Africa in particular is a region of interest for the emergence of a renewable energy supply chain between Africa and the EU.

Some of the proposed energy supply chains between Northern Africa and the EU utilize hydrogen as an energy vector. Hydrogen is relatively easy to transport and has the potential to be stored over a range of timescales. Moreover, worldwide hydrogen infrastructure is already present, as currently, it comprises about 4% of global final energy consumption. Finally, the use of hydrogen has the additional benefit of potentially decarbonizing heavy industries such as steel and cement production.

A potential risk of producing renewable hydrogen using water electrolysis is that due to the large water requirement, this method of hydrogen production may come into conflict with other uses of water consumption. In particular, the region of Northern Africa is at risk of physical water scarcity.

Moreover, the implementation of a renewable hydrogen supply chain between Northern Africa and the EU within less than 30 years will be a massive project, both in terms of investments as well as operations. Therefore, it is vital for decision-makers to have an understanding of a hydrogen supply chain in terms of costs, efficiency, and operations to be able to implement policies, laws, and other instruments to aid with implementation.

1.2. Knowledge gaps

To gain a better understanding of the envisioned energy system, literature on hydrogen supply chain network design (HSCND) is consulted. Based on this literature, several topics that are expected to influence the viability of a renewable hydrogen supply chain, specifically between Northern Africa and the EU, for example, the use and availability of water, have been examined. Four main knowledge gaps of particular interest to the region under consideration have been identified in the HSCND literature. The main challenges for designing a renewable hydrogen supply chain between Africa and the EU are the geographical scale of the system, the primary system objective, the absence of alternative storage options, and the availability and cost of water supply.

The first knowledge gap relates to the geographic scale of the envisioned system. A noticeable commonality between papers on HSCND reviewed for this work is the geographic scale of the research. Many of the research papers on HSCND consider regional or national hydrogen supply chains, however international systems including trade and transport, are often not included [18–23]. This means that transport costs are often not included on the scale required for an intercontinental supply chain. As transportation costs are dependent on the distance of transportation, longer transportation routes may have a significant contribution to the overall cost and therefore the overall economic viability of a hydrogen supply chain. Very recently, however, some studies on intercontinental renewable energy supply chains have been carried out that do take the larger geographical scale into consideration. For example, the work of Doodeman looks into a supply chain of renewable ammonia production between Morocco and the EU, or the work of Roobeek looks into a renewable hydrogen supply chain between the port of Sohar and the port of Rotterdam [24, 25].

Secondly, the primary objective of many papers looking into HSCND is to minimize the levelized cost of hydrogen (LCOH) in the overall supply chain. Since the utilization of fossil fuels for hydrogen production has historically been cheaper than the use of renewable energy, papers that include both tend to favor fossil-based hydrogen production [23, 26–28]. However, as mentioned previously, the continued use of fossil fuel-based energy is not sustainable in the long term and moreover does not align with the climate

goals. Therefore alternative hydrogen production routes are required. Although the cost of production is one of the main metrics for determining the viability of a proposed energy system, it should not be the only criterion. By focusing solely on the LCOH, other important criteria in the context of a hydrogen supply chain, for example, availability of resources and emissions reduction, may be overshadowed.

Thirdly, as pointed out by Li et al., storage is a vital part of a hydrogen supply chain network based on electrolysis using renewable electricity, in order to mitigate the effects of both short and long-term variability of hydrogen supply [18]. Although various storage options for hydrogen are present, not all hydrogen storage options are explored equally in literature. Until recently, the main technology considered for hydrogen storage was the storage of liquid hydrogen [29–35]. Underground storage of pressurized gaseous hydrogen has only gained increasing interest recently [36].

Availability and cost of water is the fourth aspect of HSCND that is underrepresented in the literature. Although water is the primary feedstock for electrolysis, many works do not explicitly represent this in their models [18]. As mentioned in Section 1, water scarcity may lead to competition between water availability for human consumption and for industrial processes, especially in arid regions such as Northern Africa. The effects of representing the water feedstock as an explicit part of the supply chain are not well-known.

1.3. Research questions

As stated previously, the main goal of the thesis is to determine the economic performance of the renewable hydrogen supply chain. The research can be summarized in the main research question presented below:

What is the economic performance of an optimal renewable hydrogen supply chain between Northern Africa and the European Union in 2050?

In order to find an answer to the main research question stated above, several subquestions are formulated that can be answered individually. Section 1.2 describes various factors that influence economic performance, but these factors are not been thoroughly researched as of yet. In this study, these factors will be included and their effect on the performance of the supply chain will be examined. As the economic performance of the proposed supply chain is based on the design of the system, the first subquestion aims to find a single system layout that will be further examined. The system layout here refers to the different processes and technologies required to produce renewable hydrogen.

- What technologies can be selected for a hydrogen supply chain producing renewable hydrogen using renewable electricity as feedstock?

In order to find the cost of hydrogen of the associated supply chain, the system must be adequately sized for the energy demand to be fulfilled, which directly impacts the required capital expenditures as well as the operational expenditures. Therefore, the following subquestions must be answered:

- What is the optimal size required for the various system components to produce renewable hydrogen at the lowest cost for the proposed supply chain design?
- What is the optimized economic performance of the proposed supply chain design?

Once the layout of the system is determined and the economically optimal design is established, the performance of the system can be examined. The economic performance can be examined by comparing the performance of the proposed supply chain to the performance of alternative hydrogen supply

chains, for example, hydrogen production using steam methane reforming with carbon capture and storage. Moreover, the economic performance can be examined by identifying the factors that influence the economic performance of the system the most, for example, a technology that has the most uncertainty in price. Therefore, the following subquestions must be answered:

- How does the economic performance of the optimal supply chain compare to alternative energy supply chains?
- What factors that affect the economic performance of the proposed supply chain can be identified?

1.4. Thesis scope and goals

The main goal of this work is to gain a better understanding of large-scale renewable hydrogen production in Northern Africa, by performing an economic analysis using optimization modeling. This is exploratory research, which focuses on finding the performance of an optimized supply chain layout and operations of an international hydrogen production route. As presented in Section 2.2, this work assumes a simplified system layout, consisting of renewable energy generation, water purification, electrolysis and hydrogen storage and distribution. Transport routes between the various echelons in the system are examined on a general level.

As this is exploratory research, the focus of the work is on finding the factors that impact the economic performance of a large-scale renewable hydrogen supply chain. By modeling the various echelons of the proposed supply chain and applying a case study, the performance of the supply chain is determined. This research distinguishes itself from previous research by the inclusion of both water feedstock as a separate echelon as well as including underground storage of hydrogen.

One of the main goals regarding the model is to build it keeping generality in mind. Although the focus of this work is on a specific case study, the model should be able to be adapted to a different case study by varying case-specific model parameters. This allows the model to analyze various case studies using the same modeling methodology. Moreover, keeping the model general allows other users to implement additional features in the model if required. The model will be built as an optimization problem, aiming to optimize for economic performance, which in this context will be to minimize the costs.

1.5. Research approach

This section will describe the approach that is taken in order to answer the research questions stated in Section 1.3. First, the general system design is determined using previous literature on the topic of hydrogen supply chains. Next, a brief literature review on the various system echelons is performed, to gain an insight into the technologies currently available for performing the echelon functions. For the chosen technologies, literature studies are consulted to find the technical and economic parameters required to solve the model, for example, the cost of a photovoltaic (PV) system.

Furthermore, an optimization-based model of a hydrogen supply chain is set up in Python using the Pyomo library. The supply chain echelons and the various interactions between them are mathematically modeled in a mixed integer linear programming model, aiming to minimize the total annual cost of the overall supply chain. The technologies determined by the literature review are combined into a specific case study. This case study is then included in the model in order to be able to solve it. The economic and technical parameters of the technologies described by the case study are adapted from the literature. The model is then solved using Gurobi, solving for the optimal size of the plants, optimal

flows of mass and energy between the plants, and the distribution routes of these flows. By doing this optimization, not only is the supply chain investigated, but also the network of the supply chain between the countries present in the case study.

After the case study is solved, a comparison is made between the results of this case study and previous literature. This comparison is then used to draw conclusions on the viability of the overall supply chain and to give recommendations on the crucial factors of the supply chain.

1.6. Thesis outline

In Section 2, previous literature related to this work is described, the system layout for this thesis is presented and background information on the various system echelons is given. Next, in Section 3 the formulation of the optimization model is presented. In Section 4 the case study is presented, and the parameters used in the model are discussed. In Section 5 the results of the case study are presented. In Section 6 the results are discussed and, finally, in Section 7 the answer to the main question, conclusions of this work, and recommendations for future research are discussed.

2

System design

This section provides an overview of the renewable hydrogen supply chain system used in this research. First, a general description of the system and system components is given. Next, the technologies associated with each of the echelons are described in more detail. This description will include the working principles of the technologies as well as some advantages, disadvantages, and technical challenges of the technologies. Finally, the layout of the echelons within the system is discussed.

2.1. System description

A hydrogen supply chain generally contains feedstock, production, transportation, and distribution, and often but not always some form of storage [18, 37, 38]. In the case of a renewable hydrogen supply, the feedstock is generally assumed to be renewable electricity, with water electrolysis as production.

For the research to be conducted in this thesis a renewable hydrogen supply chain is considered, starting with the production of raw materials and ending with material import. The supply chain determined for this work is shown in Figure 2.1.

The supply chain starts with a solar power plant generating electricity as primary energy feedstock. The electricity is then transported via AC powerlines to the water treatment plant as well as to the electrolysis plant. Water is supplied from the water treatment plant, acting as second feedstock, and transported through pipelines to the electrolysis plant. In the electrolysis plant, hydrogen is produced. The produced hydrogen is then transported via pipeline to the storage facility, where it is stored until the hydrogen is transported to demand, and two hydrogen demand sites that both cover half of the total yearly hydrogen demand.

In the proposed supply chain, all echelons required for renewable hydrogen production are taken into account and are assumed to be non-existing as of today. All infrastructure required for the supply chain needs to be newly built. Opposed to previous research, in this work the water feedstock is an integral part of the supply chain, as water availability can be a bottleneck in future renewable hydrogen production.

As mentioned in Section 1.4, this thesis aims to find the economic performance of a renewable hydrogen

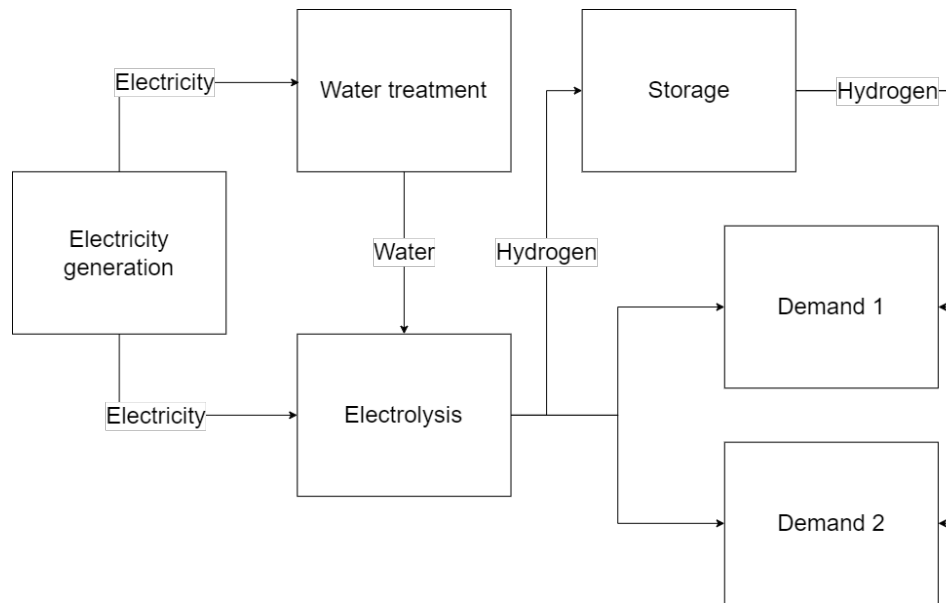


Figure 2.1: Schematic representation of the hydrogen supply chain under consideration.

supply chain, specifically between Northern Africa and the EU. The performance of this supply chain will be evaluated by a model that is set up for this thesis. The formulation of the model will be further elaborated on in chapter 3. In this section, a basic description of the system under consideration for the case study is discussed. In chapter 4, the parameters used to describe the case study are described.

The proposed supply chain is located in Morocco, the Netherlands, and Poland. The location of each echelon is presented in Figure 2.2. Based on a multi-criterion approach in the work of Smale, Morocco is chosen as one of the prime starting points for the supply chain under consideration [39]. Poland and The Netherlands are chosen to simulate hydrogen demand for both eastern and western Europe respectively. Additionally, the Netherlands allows for storage in underground salt caverns as well as depleted gas fields.

The echelons required for renewable hydrogen production are all present in Morocco. The solar plant, shown by the yellow marker, is located in a desert region near Marrakesh. The water required for hydrogen production is extracted from seawater. The water treatment plant is located near Essaouira, a small city bordering the Atlantic ocean, shown in blue. Finally, the electrolysis plant, shown in orange, is located in Marrakesh, in between the electricity generation and water treatment plants.

Storage of hydrogen in the supply chain is located in the EU. More specifically, the hydrogen will be stored in Groningen, the Netherlands, as shown in green in Figure 2.2. As the main purpose of the supply chain is to provide the EU with renewable energy in the form of hydrogen, two demand sites, marked in red, are placed within the EU. The demand sites are located in the Netherlands and Poland, to stimulate demand for both eastern and western Europe. For simplicity, it is assumed all storage and demand sites are connected to the transport network. However, realistically these connections are only present if the echelons are already part of the existing gas infrastructure.

The distance between each echelon is calculated using the haversine function as the arc length between two points on a sphere. Although this is a realistic first-order approximation of transport distance, this method fails to include harder-to-model natural barriers. For example, the connection between electrolysis in Morocco and demand in Poland crosses straight through the Mediterranean Sea and

the Alps. In reality, the transport distances between echelons are expected to be larger than modeled. For simplicity, only the utilization of transport connections between various echelons is considered. Although the capacity of the transport connections determines the overall amount of transported water, electricity, and hydrogen, the capacities of transport networks are not taken into account in this work.

The supply chain described above will be analyzed using the model described in chapter 3. The main point of interest of the case study is to find the optimal sizes of the various system components, based on a given demand. The supply of electricity is based on the amount of solar irradiation present at the location of the solar plant. Next, the flows of mass and energy between echelons are determined and used to find the transport strategy between the echelons. Furthermore, the behavior of the storage site is analyzed. The behavior of the system is guided by optimizing the system for minimization of the overall yearly costs of operating the supply chain.

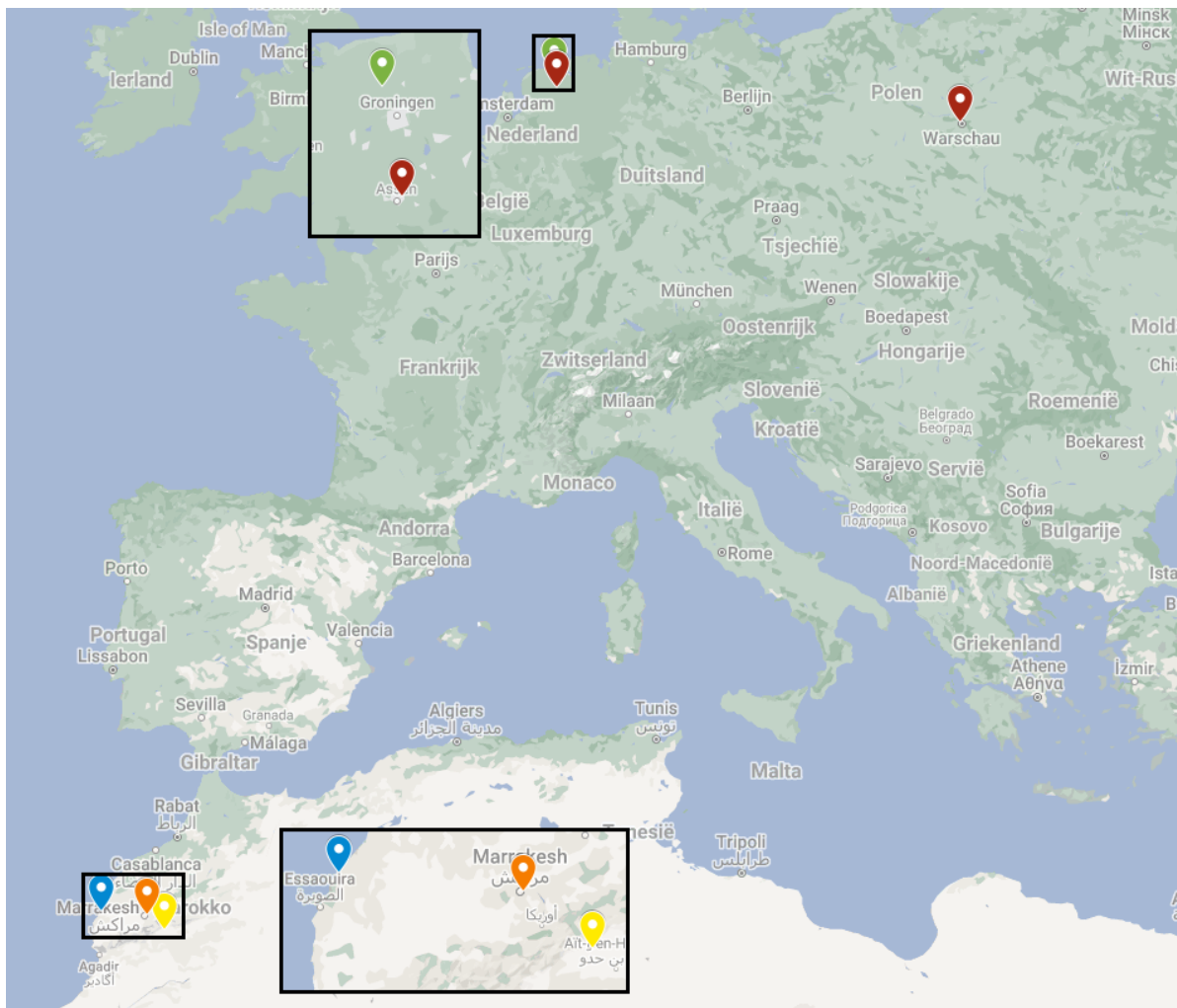


Figure 2.2: System layout of the supply chain model. Echelons are colored yellow (solar plant), blue (water treatment), orange (electrolysis), green (storage), and red (demand).

2.2. Technology selection

In the previous section, a general description of the supply chain used for the case study is presented. The performance of the supply chain is, however, dependent on the technologies that are assumed in the case study. The following sections provide an explanation of the technologies selected for the

case study. For each echelon, a description of the working principles of the technologies considered is given and the selection choices are elaborated on. This section starts with the production echelons; electricity-, water- and hydrogen generation, followed by storage and transportation of hydrogen.

2.2.1. Electricity generation

The electricity generation echelon of the system is responsible for producing the electricity required to operate the overall supply chain. Solar PV technology is proposed to be the primary supplier of renewable energy for the supply chain, due to the maturity of the technology, widespread use and manufacturing of the technology, and the favorable weather conditions at the selected location. The rest of this section will describe solar PV technology in more detail.

PV technology directly transforms photons into electricity according to the photoelectric effect [40]. A solar cell consists of two layers of semiconductor material, where one side is negatively doped and one side is positively doped [41]. At the p-n junction, the boundary between the two semiconductor materials, excess charge carriers diffuse, giving rise to an electrical field between the two layers. When the photon energy of light is absorbed by the solar cell, charge carriers are migrated through the semiconductor material, resulting in a voltage difference over the solar cell. If at this time, the electrical circuit within the solar cell is closed, an electrical current will flow. The above-mentioned process is shown in Figure 2.3.

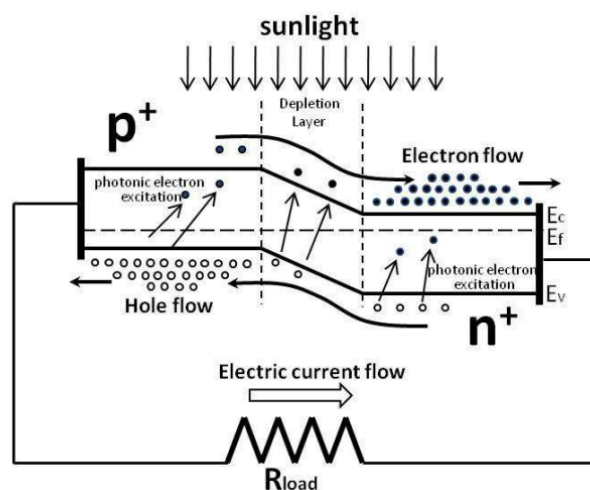


Figure 2.3: Illustration of the working principle of a solar cell based on a p-n junction under the presence of an external photon source. Retrieved from [42].

In order for the energy of a photon to be absorbed by the solar cell material, the photon energy must be higher than the bandgap energy of the material, which is the difference between the lowest energy of the conduction band and the highest energy of the valence band [43]. The band energy for a given material is constant, hence the bandgap energy for any two given semiconductor materials is always the same, with the exception of a slight temperature dependence. Whenever the photon energy is the same as the bandgap energy, exactly one electron is excited and a single electron-hole pair is created. When the photon energy is higher than the bandgap energy, some of the photon energy is converted into heat, resulting in a slight loss of energy.

The amount of energy that is converted in a solar cell is thus dependent on the bandgap energy between the two semiconductor materials. Whenever the bandgap is relatively low, more low-energy photons

are able to excite electrons, resulting in a broader range of photon energies able to be absorbed. However, low bandgap energy also results in thermal losses for high-energy photons. On the other hand, when the bandgap energy is high, less photons can be absorbed, but the energy losses of the absorbed photons are small. In order to maximize the conversion efficiency of a solar cell, the bandgap energy of the cell must be somewhere between these two extremes.

Currently, several solar cell technologies exist, which are most commonly divided into mono-crystalline, poly-crystalline, and thin-film solar cells [44]. Mono-crystalline solar cells consist of a single silicon crystal and are currently the most widespread PV technology. However, due to the production process, mono-crystalline solar cells tend to be expensive. Poly-crystalline solar cells consist of multiple crystalline silicon grains as a way of reducing manufacturing costs. Since poly-crystalline cells consist of multiple grains, these cells inherently have multiple boundaries, resulting in a lower efficiency compared to mono-crystalline solar cells. The final solar cell technology is thin-film solar cells. As the name suggests, thin-film solar cells are designed to be as thin as possible. The main advantage of thin-film solar cells over mono- and poly-crystalline solar cells is the reduced amount of required material to create the solar cell, with the aim of lowering the costs of solar cell production.

The efficiency of solar cell configurations is not only dependent on the technology used, but also on the deployment and operation strategy, which dictates the azimuth and elevation angle. The azimuth angle is the angle of the solar panels relative to the equator. The elevation angle is the angle of the system relative to the ground. The optimal deployment of a solar system is to directly let it face the sun. On a daily timescale, this means the optimal azimuth angle changes throughout the day, as the earth rotates around its axis, changing the location of the sun relative to the earth. On a seasonal scale, due to the tilt of the earth, the height of the sun relative to the sky changes over time, resulting in a change in optimal elevation angle throughout the year.

There is a distinction between operating modes for PV systems. Small-scale applications often utilize a fixed assembly, where the azimuth and elevation angle is fixed. PV-tracking systems follow the path of the sun and are more efficient compared to fixed PV systems, but these systems do require more land area. Moreover, part of the electricity produced is required for moving the solar panels themselves. For the purposes of this work, it is assumed that a fixed solar panel layout is used. Although this is less efficient, it is both cheaper and easier to install and operate. The technology that is used in the supply chain model is poly-crystalline solar cells. Currently, this is the cheapest technology able to be mass-produced, making this technology the most viable option for large-scale applications.

2.2.2. Water purification

Current technologies for water electrolysis rely on ultra-pure fresh water [45]. Freshwater, however, is scarce, at approximately 1% of the global water reserve. In order for large-scale widespread electrolysis to be viable without compromising the freshwater supply for alternative primary uses such as human consumption and agricultural use, using seawater as a water supply is thought to be a possible alternative. Not only would this reduce the levels of water stress in arid regions, but producing the required water feedstock within the supply chain would also reduce the dependency on the availability of a freshwater source near the electrolyzer. This would also allow water electrolysis to be a possible solution for long-term electricity storage in remote locations, for example, islands.

In order for seawater to reach the purity required for current electrolyzer technologies, microorganisms, sediment, and several ionic species must be removed from the water [45]. Both sediment and

microorganisms can be removed from seawater by filtration pre-treatment [45]. Ionic species, however, must be removed using other technologies, as they are dissolved in the water and can therefore not be filtered out easily [45].

Desalination technologies are classified under thermal processes, membrane processes, and alternative processes [46]. Each of these processes is summarized below:

1. Thermal processes utilize distillation in order to desalinate seawater. Technologies for thermal desalination include multi-stage flash distillation (MSF), multi-effect distillation (MED), and vapor compression distillation (VCD).
2. Membrane processes utilize semi-permeable membranes to separate water from contaminants. Technologies include reverse osmosis (RO), electro-dialysis (ED), and membrane distillation (MD).
3. Alternative processes are currently under development, but have not yet reached commercial maturity [47]. Examples are freezing desalination and ion exchange membrane desalination. For the purposes of this work, these alternative desalination technologies are not taken into consideration, due to the immaturity of the technologies and the high long-term economic uncertainties.

As mentioned, thermal processes rely on the distillation of seawater for desalination. MSF and MED are very similar technologies, and both operate by pressurizing and heating seawater through multiple stages of distillation. The main difference between MSF and MED is in the use and re-use of heat in the system [46, 47]. In MED, the pressure in subsequent vaporization chambers is lower, which allows the water vapor in one chamber to provide the heat for the subsequent vapor, which in turn improves the overall process efficiency and reduces energy consumption per unit of desalinated water produced, compared to MSF. VCD is a desalination technique where the heat of vaporization is provided by vapor compression using mechanical or thermal compressors [46]. Incoming seawater is used to cool down the vapor stream, which simultaneously results in the seawater stream heating up. Due to higher capital and maintenance costs, however, VCD sees less widespread use compared to MSF and MED.

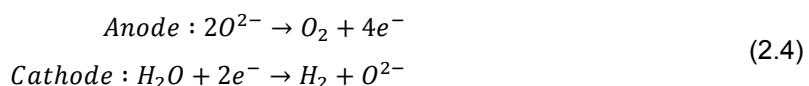
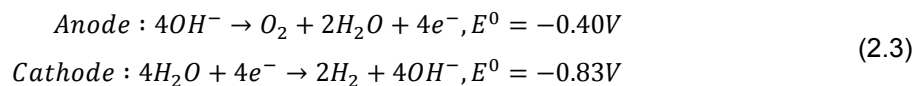
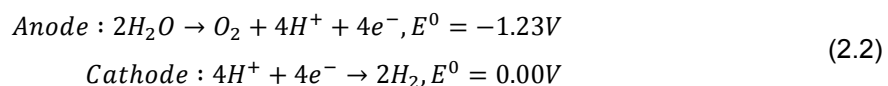
Membrane water treatment methods all work on similar principles, where a (semi-)permeable membrane is used to separate water and its contaminants into two separate regions [47]. The difference between various technologies mostly lies in the size of the membrane pores, which dictate what species are separated. Next to this, the driving force for separation differs between various technologies and can be provided by a difference in temperature, pressure, or electrical potential [48]. RO works by forcing pressurized salt water through a separation membrane. In order to prevent membrane fouling, RO requires pre-treatment of the feed water in order to remove large particles. In ED, the driving force for separation is an electrical potential difference. Ionic species are allowed to pass through the membranes towards the side with an opposite electric charge. MD is a technology where thermal and membrane processes are combined. The driving force of MD is a temperature difference, that results in a higher vapor pressure of water at one side of the membrane. The hydrophobic membrane only allows for water vapor to pass through, which is then condensed on the other side.

Since membrane water treatment technologies require less energy per unit of desalinated water, for the purpose of this thesis it is assumed that only membrane technologies are used. More specifically, only the use of RO is assumed. Although pre-treatment is required for the use of seawater in RO, the energy requirement for pre-treatment is only small compared to the overall energy input of RO. RO does have significant advantages over alternative desalination methods for the purposes of this work.

RO only has demand for electrical energy, requires relatively low investments, and is demonstrated to be suitable for coupling with renewable energy sources [49]. Furthermore, RO is a relatively new technology compared to thermal water treatment technologies, implying more room for improvement in the near future.

2.2.3. Electrolysis

Water electrolysis is the process of dissociating water molecules into hydrogen and oxygen. The reaction associated with this process is presented in Equation 2.1. The dissociation of water is a redox reaction, where electrons are transferred from the oxygen atom onto the hydrogen atoms. The redox couples present in this reaction are H_2O/H_2 and H_2O/O_2 . In principle, there are two pathways of water dissociation using electrolysis, depending on whether the reaction medium is acidic or alkaline. The half-reactions for both pathways are shown in Equations 2.2 and 2.3 for acidic and alkaline media respectively [50]. At high temperatures, water can be dissociated directly into hydrogen and oxide ions. This is shown in Equation 2.4.



At standard temperature and pressure (STP, $T^0 = 298K$, $P^0 = 1 \text{ bar}$), the state of matter for water is liquid, and for hydrogen and oxygen is gaseous. The thermodynamic properties associated with the dissociation of water are presented in Table 2.1. As the Gibbs free energy change for the dissociation of water is positive, the reaction is non-spontaneous, and an external energy source is required to drive the reaction [51]. In water electrolysis, electricity is the external energy source and is converted into chemical energy and heat during the reaction.

Table 2.1: Thermodynamic properties for reaction 2.1

Property	Symbol	Value	Unit
Enthalpy	ΔH^0	+285.84	kJ mol^{-1}
Entropy	ΔS^0	+163.15	$\text{J mol}^{-1} \text{K}^{-1}$
Gibbs free energy	ΔG^0	+237.22	kJ mol^{-1}

The thermodynamic properties presented in Table 2.1 all have a temperature and pressure depen-

dence. Therefore, if electrolysis is not performed at STP, the thermodynamic equilibrium conditions for the reaction change. Assuming that the reaction takes place in near-equilibrium conditions, the temperature and pressure dependence of the reaction is described through the Gibbs-Helmholtz equation as shown in Equation 2.5 [51]. The temperature dependence on the thermodynamics of water dissociation can be intuitively understood from Equation 2.5. As the temperature at which the reaction takes place increases, the entropic term increases, and therefore the Gibbs free energy decreases. This results in a lower demand of electric energy for water dissociation at higher temperatures, as shown in Figure 2.4.

$$\Delta H(T, P) = \Delta G(T, P) + T\Delta S(T, P) \quad (2.5)$$

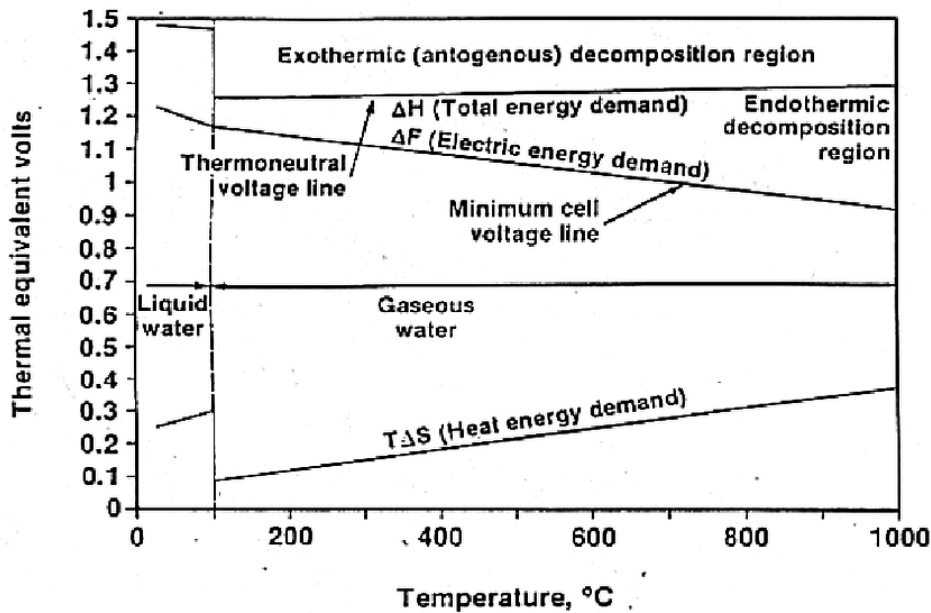


Figure 2.4: Thermodynamics of water electrolysis. Retrieved from [52]

Electrolysis of water is carried out in an electrochemical cell. A basic electrochemical cell contains two electrodes, an anode, and a cathode, some form of barrier between the electrodes that allow the transport of ions and a connection between the anode and cathode to close the circuit.

As of now, there are three main technologies that can perform electrochemical dissociation of water. These are polymer exchange membrane electrolysis (PEM), alkaline electrolysis (AEL), and solid oxide electrolysis (SOEL). The various electrolysis technologies differ in cell design and operation conditions. In the next sections, the different technologies are shortly elaborated on.

AEL: In AEL, water dissociation is performed with the electrodes submerged in an alkaline solution, and the half-reactions as shown in 2.3 apply. The electrodes in an AEL cell consist of non-noble metals, such as nickel and iron, making AEL cells relatively affordable. The electrodes are in contact with the electrolyte, consisting of a concentrated solution of lye, often as KOH. Between the electrodes, a diaphragm is present that allows for the migration of hydroxyl (OH^-) ions, but has only limited permeability towards hydrogen and oxygen gas. The diaphragm, therefore, acts as both a medium for the migration of charge-carrying particles, as well as a barrier between the product streams.

PEM: The enabling technology for PEM electrolysis is the proton-conducting membranes. The utilized

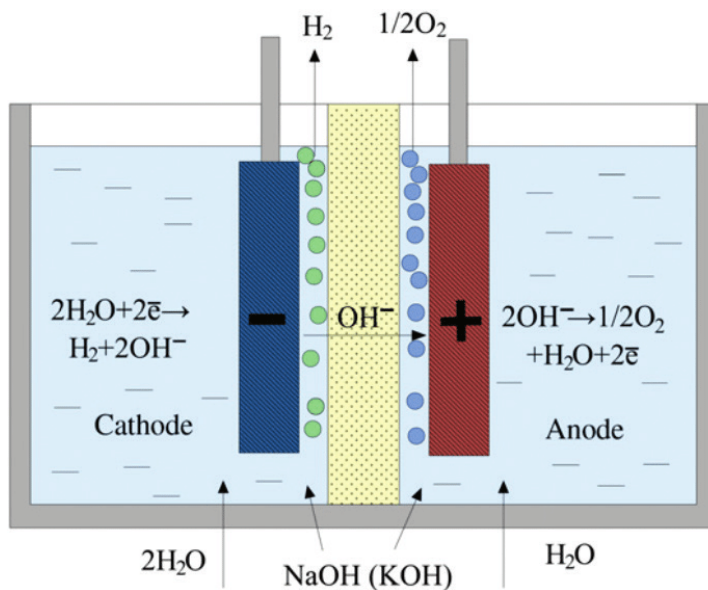


Figure 2.5: Schematic representation of an alkaline electrolyzer. Retrieved from [53]

polymer membranes allow for the exchange of protons, but have low permeability for the exchange of gasses. Due to the corrosive nature of PEM electrolysis, materials suitable for building the cells are limited. As a result, electrodes often consist of platinum group catalysts, such as iridium, that are significantly more costly compared to AEL electrodes [51, 54]. At the anode, water is oxidized into oxygen gas and protons. The protons then migrate through the polymer membrane to the cathode, where the reduction of protons into hydrogen gas takes place [54]. In Figure 2.6 a schematic representation of a PEM cell is shown.

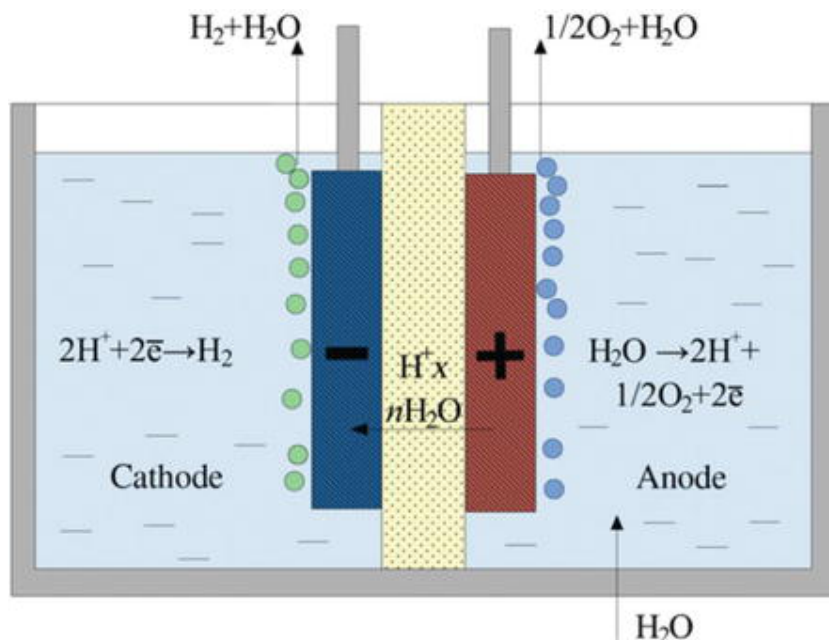


Figure 2.6: Schematic representation of a PEM electrolyzer. Retrieved from [53]

SOEL: High-temperature electrolysis, in contrast to its competing electrolysis technologies, is carried out at temperatures between 700 and 900 °C. In SOEL, the half-reactions as described in Equation

2.4 apply. The oxide ions that are formed at the cathode migrate through the solid electrolyte, where they are oxidized into oxygen gas. The electrolyte material consists of zirconium oxide (ZrO_2) doped with yttria, scandium oxide (ScO_2) or cerium oxide (CeO_2) [55]. The cathode consists of a composite material made from approximately 40 vol.% nickel and 60 vol.% electrolyte material. For the anode, perovskite-structured mixed ionic and electronic conductor materials are used, for example, lanthanum strontium cobalt ($La_{1-x}Sr_xCoO_3$) or lanthanum strontium cobalt ferrite ($La_{1-x}Sr_xCo_{1-n}Fe_nO_3$) [55, 56]

A comparison of technical parameters is made for the three types of electrolyzer technologies as described above. A summary of this comparison is shown in Table 2.2 below.

Table 2.2: Summary of parameter comparison between AEL, PEM, and SOEL ([57–59]).

	AEL	PEM	SOEL
Operational parameters			
Temperature ($^{\circ}C$)	60-90	50-80	700-900
Pressure (bar)	10-30	20-50	1-15
Current density (A/cm^2)	0.20-0.45	1.0-2.0	0.3-1.0
Flexibility			
Cold start-up time (min)	60-120	5-10	> hours
Warm start-up time (s)	60-300	< 10	> 900
Load flexibility (% of nominal load)	20/100	0/100	-100/100
Efficiency			
Nominal system efficiency (% of LHV)	50-60	46-60	76-81
Energy consumption (kWh/Nm^2)	5.0-5.9	6.0-6.5	3.7-3.9
Durability			
Lifetime (kh)	50-120	60-100	8-20
Efficiency degradation (%/y)	0.25-1.5	0.5-2.5	<0.06

For the purposes of this thesis, only low-temperature water electrolysis is assumed to be used in the renewable hydrogen supply chain. Although SOEC has some favorable properties such as high efficiency, low electricity consumption, and large load flexibility, the high-temperature operating conditions are not suited for the proposed system as a secondary power source would be required in order to keep the SOEL cells under operating conditions at times where electricity supply from the main power generation facilities is insufficient. The remaining low-temperature electrolysis technologies have several advantages and disadvantages compared to each other.

Both AEL and PEM have similar lifetimes. The technological advantages of PEM over AEL are the higher current densities, lower start-up and ramp-up times, and higher load flexibility. Moreover, PEM operates at higher pressures, reducing the need for pressurization after hydrogen production. In contrast, AEL operates at higher temperatures, resulting in higher electrical energy efficiencies and in turn lower electrical energy consumption. In this work, the main technology assumed for electrolysis is AEL, mainly due to the favorable cost of AEL compared to PEM, due to the use of common materials for the electrodes.

2.2.4. Storage

Storage is required for any supply chain that operates under temporal variation of supply or demand and is not exclusive to energy systems. The main function of storage is to maintain the smooth distribution of goods in non-continuous systems. For example, a factory warehouse stores goods until the goods are bought and shipped. In an energy system, storage serves a similar purpose. For example, at oil terminals, oil is supplied in batches, whereas the oil refineries operate continuously in order to maximize

the capacity factor. In the following section, background information for the storage of hydrogen is presented.

There are various ways to store hydrogen, but most often it is stored as a compressed gas. Other options include storing hydrogen as a liquid, in liquid hydrogen carriers, or as metal hydrides. Due to the scale of the required storage, in the thesis only compressed hydrogen storage is taken into account. Hydrogen is often stored as a compressed gas, since this reduces the required storage volume. Under STP conditions, the density of hydrogen gas is 0.0813 kg/m^3 , whereas the density of hydrogen at a similar temperature under a pressure of 10 MPa is 7.67 kg/m^3 [60]. This effect is also shown in Figure 2.7 below. However, compressing hydrogen to reduce storage volume requires work, reducing the overall efficiency of the storage system.

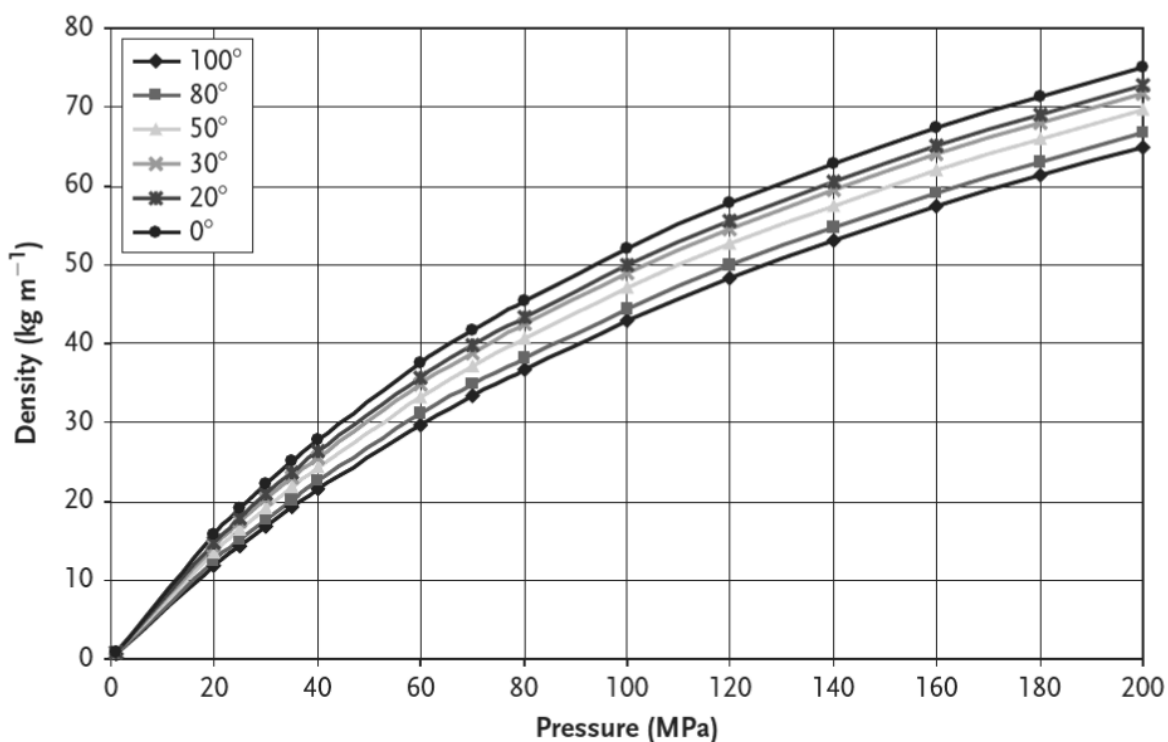


Figure 2.7: Pressure and temperature dependence on the density of compressed hydrogen gas. Retrieved from [61]

In this thesis, it is assumed that the full storage capacity for compressed hydrogen is fulfilled by underground hydrogen storage, specifically in salt caverns. Cavern storage is able to provide long-term storage for hydrogen at volumes comparable to production capacity [62, 63]. From a technological perspective, underground storage of hydrogen is similar to the storage of natural gas, which has been done for hundreds of years [64]. Storage of hydrogen in salt caverns is a promising technology for several reasons. First, the costs associated with hydrogen storage in salt caverns are lower compared to conventional storage tanks [63, 64]. Next, underground storage of hydrogen is less susceptible to safety hazards such as fire [63–65]. Furthermore, underground hydrogen storage requires relatively little land area [65, 66].

Salt caverns have some advantages over other types of underground hydrogen storage, for example, aquifers or porous rocks, due to their material properties. Hydrogen in underground hydrogen storage is susceptible to microbial effects, resulting in the formation of methane or hydrogen sulfide [67]. Salt caverns are expected to have a much lower risk of microbial activity compared to porous rocks, for two

main reasons [67]. First, salt caverns have a significantly lower surface area compared to porous rocks, reducing biofilm formation and clogging. Second, the diversity and abundance of microorganisms is reduced by the saline environment. Next to the microbial effects, salt caverns also have low permeability, reducing leakage of hydrogen, which not only improves system efficiency but also reduces hazards [68, 69].

3

Approach

In section 2.1 a general description is given of the supply chain is analyzed. In order to analyze this supply chain, a model is created. This chapter provides an overview of the mathematical description of this model. First, a general overview and introduction to the model are given. Next, the model is explained and elaborated on by providing the mathematical formulation of the model. Finally, metrics used to evaluate the system performance are defined.

3.1. Model overview

In order to determine the optimal supply chain configuration, a model is set up that determines the optimal plant sizes, the location of transport connections, and the mass and energy flows between plants. The model is built in python, using the Pyomo library to write the optimization model and Gurobi to solve the resulting system. The model is simulating the operation of the supply chain for one full year, with a time resolution on a monthly scale, resulting in twelve distinct time slots. The model runs on an AMD Ryzen 5 3600 with a 3.6 GHz frequency. Using Gurobi as the model solver enables the use of multi-core threading, resulting in the use of twelve threads on the aforementioned CPU. This means Gurobi is able to perform parallel calculations, reducing the overall calculation time compared to single-thread calculations. The computation time for the model using the described setup is approximately 0.00 seconds.

The optimization model set up for this research only has linear expressions and can therefore be classified as a Linear Program (LP). Furthermore, continuous as well as discrete variables are present in the model, therefore the model can be classified further as a Mixed Integer Linear Program (MILP). Two components are present in the formulation of a MILP, the objective function, and the constraints.

In this work, the optimization objective is to minimize the total annual costs of the overall supply chain. The echelons that are represented in the model are power generation, water purification, electrolysis, transport, and storage. The main aim of the model is to find the required sizes of, and the mass and energy flows between system components.

For this purpose a general model is set up that will be further elaborated in section 3.2. Generality in

this context means that the model is not specific to the case study, but rather a general model for any hydrogen supply chain. The model uses a black-box approach for the echelons, where the internal system processes are not modeled in detail. The specific type of technologies implemented in the model are determined by the technical parameters defined for each echelon, which can be varied for other case studies.

Model notation

Sets

T	Time	[Months]
I	Echelon index of sending plants	
J	Echelon index of receiving plants	
G	Goods	

Subsets

$I^p \subset I, J^p \subset J$	subsets containing all power plants
$I^w \subset I, J^w \subset J$	subsets containing all water treatment plants
$I^e \subset I, J^e \subset J$	subsets containing all electrolysis plants
$I^s \subset I, J^s \subset J$	subsets containing all storage plants
$I^d \subset I, J^d \subset J$	subsets containing all demand sites

Parameters

γ_{LHV}	Lower heating value of hydrogen	[kWh/kg]
γ_{H_2O}	Required mass of water to produce one unit of hydrogen	[kg]
η_i	Efficiency of echelon i	[-]
c_w	Production cost of one unit of water in plant i^w	[\$/m ³]
D_t	Demand at time t	[TWh]
$d_{i,j}$	Distance between echelon i and j	[km]
$E_{irr,t}$	Irradiation at time t	[kWh/m ² /day]
M_0	Initial storage amount across all storage sites	[TWh]
$M_{i,max} \forall i \in I^s$	Maximum amount of storage available in echelon i	[TWh]
$M_{i,min} \forall i \in I^s$	Minimum amount of storage available in echelon i	[TWh]
r	Interest rate	[%]
$V_{storage}$	Total storage volume	[TWh]

Model variables

$A_{t,r}$	Annuity of a plant with lifetime t and discount rate r	[-]
EAC_i	Equivalent Annual Cost for plant i	[\$/yr]
$D_{i,t}, \forall i \in I^d$	Hydrogen demand of plant i at time t	[TWh]
$E_{i,t}$	Electrical energy output of echelon i at time j	[TWh]
$M_{i,t}, \forall i \notin I^s$	Hydrogen output of echelon i at time t	[TWh]
$M_{i^s,t}, \forall i \in I^s$	Hydrogen present in echelon i^s at time t	[TWh]
NPV	Net present value	[\$]
$OPEX_i$	Operational expenditures of plant i as percentage of CAPEX	[%]
TAC_i	Total Annual Cost for plant i	[\$/yr]

Decision variables

$E_{i,j,t}$	Electrical energy distributed from echelon i to echelon j at time t	[TWh]
$M_{i,j,t}$	Hydrogen distributed from echelon i to echelon j at time t	[TWh]
n_i	Size of echelon i	[GW, m ³ /day]
$TN_{i,j,g}$	Utilization of a transport network between echelon i and j for a good g .	[0,1]

3.2. Optimization model

The optimization model can be represented as the combination of sets, parameters, constraints, and the objective function that together represent the full system within the system boundaries. Sets provide the indices for parameters, proving to be useful in generating expressions in python that resemble the mathematical formulation more closely. Constraints define relations between variables and coefficients within the model. The objective function dictates the objective of the model, determining what variable is to be optimized.

Given some pre-determined plant locations, as presented in section 2.1, supply and demand data, and technology parameters regarding efficiency and cost, the model identifies the optimal design for hydrogen production as well as the system operation in terms of mass and energy flows between the various echelons. The model determines the size of system echelons, the utilization of long-term storage as well as the presence and location of the transport network.

In the proposed optimization model there exist four sets that define the indices used in the formulation of mathematical expressions. The length of each set is determined by the number of values within each set. As the sets in the model all start at index 0, the final index value of each set is equal to the number of values minus one. The first set is concerned with making time discrete.

$$t \in T = \{1, 2, \dots, t_n\} \quad (3.1)$$

The other sets are concerned with indexing the various plants and are shown in Equations 3.2 - 3.3. The sets I and J represent the unique index for every plant inside of the model. The set I allows for specifying a specific plant in the system. The combination of sets I and J allows for defining variables that interact with both plants i and j . In order to properly formulate the mathematical model, and keep the formulation of the model general, it is easiest to introduce here the partition of the sets I and J .

$$i \in I = \{1, 2, \dots, n_p - 1\} \quad (3.2)$$

$$j \in J = \{1, 2, \dots, n_p - 1\} \quad (3.3)$$

Partitioning the sets I and J requires dividing the sets into finite subsets where each element in I or J is part of one, and only one of these subsets. As the sets I and J are copies, they are partitioned similarly. The subsets for I are based on the echelons present in the model, where a subset is made for every plant within the system that performs a similar function. In this model, a subset is defined for power generation I^p , water treatment I^w , electrolysis I^e , and storage I^s .

To make the partitioning more clear, the specific partition of set I for this thesis is presented below in Equations 3.4 to 3.9. The same partition holds for set J as this is a copy of I .

$$I = \{1, 2, 3, 4, 5, 6\}, \quad (3.4)$$

$$I^p = \{1\}, \quad (3.5)$$

$$I^w = \{2\}, \quad (3.6)$$

$$I^e = \{3\}, \quad (3.7)$$

$$I^s = \{4\}, \quad (3.8)$$

$$I^d = \{5, 6\} \quad (3.9)$$

As can be derived from Equations 3.4 to 3.9, the subsets contain each element of I , and every element of I appears only once in the subsets. In the general case of the model, as long as the number of subsets of I is finite, the set I can have an infinite amount of elements. In practice, this means that in the model, any amount of plants within a certain subset can be generated while keeping the exact same model formulation. For example, instead of modeling the power generation plants as one big solar plant, one could model it as a set of individual smaller plants, and the model would still hold.

The final set in the model contains all goods that are able to be transported in the model. This set is denoted by G and is defined by Equation 3.10. The goods for this case study are electricity, water, and hydrogen, but more goods can be included in the model.

$$g \in G = \{g_0, g_1, \dots, g_n\} \quad (3.10)$$

3.2.1. Objective function

At the core of the optimization model is the objective function, as it dictates what the model is optimizing. In this research, the objective function is to minimize the total annual costs of the overall system, where the total annual costs are defined as the linear combination of the total annual costs of all echelons within the system. The objective function is formulated in Equation 3.11.

$$\min TAC = \sum_I TAC_i \quad (3.11)$$

The total annual costs of the system echelons are calculated as the sum of the equivalent annual cost (EAC) and operational expenditures. Using the EAC allows the model to simulate the operation of the supply chain for a single year while taking into account the cost of capital over the lifetime of the required technologies. The EAC is defined as the net present value (NPV) of an investment over the annuity ($A_{t,r}$) factor of the investment, as shown in Equation 3.12 [70]. The annuity factor is the sum of all discount factors for the duration of the investment and is a function of both the interest rate and the lifetime of an investment, as shown in Equation 3.13.

$$EAC = \frac{NPV}{A_{t,r}} \quad (3.12)$$

$$A_{t,r}(t, r) = \frac{1 - (1 + r)^{-t}}{r} \quad (3.13)$$

In this approach, it is implicitly assumed that the yearly operational expenditures do not change over time. The TAC is then defined as the sum of the CAPEX and OPEX, where the CAPEX is represented by the EAC.

$$TAC_i = EAC_i + OPEX_i \quad (3.14)$$

The TAC_i is calculated differently for the various echelons, as the operational expenditures, as well as the plant lifetimes, vary between technologies. The next section provides an overview of the cost calculations for the individual echelons within the model. First is the cost of power generation and the electrolyzer. The costs of these echelons are directly proportional to the size of these systems and are defined by Equations 3.15 and 3.16 respectively. In these Equations, the EAC_i are defined in terms of $[cost/installedcapacity]$, therefore, the EAC_i are multiplied by the installed capacity to find the cost. For the PV and electrolyzer systems, the OPEX is defined as a fixed percentage of the CAPEX.

$$TAC_{ip} = n_{ip} \cdot EAC_{ip} + OPEX_{ip} \quad (3.15)$$

$$TAC_{ie} = n_{ie} \cdot EAC_{ie} + OPEX_{ie} \quad (3.16)$$

For the water production cost a similar approach is used, however, the costs now scale not only with the installed capacity, but also with the amount of water produced. The TAC of water production is represented in Equation 3.17, where n_{iw} represents the size of the water plant and EAC_{iw} the CAPEX. The OPEX for water treatment is different from power production and electrolysis, as the OPEX is now not a fixed percentage of CAPEX, but a linear function of the amount of water produced, as shown in Equation 3.18, where c_{iw} denotes the cost of producing one unit of water.

$$TAC_{iw} = n_{iw} \cdot EAC_{iw} \cdot OPEX_{iw} \quad (3.17)$$

$$OPEX_{iw} = c_{iw} \cdot \sum_j M_{iw,j,t} \forall t \in T, i \in I^w \quad (3.18)$$

For hydrogen storage, the costs are determined based on the size of the storage facility, similar to the cost calculations for the power generation and electrolyzer echelons. The cost calculation for storage is defined in Equation 3.19, and is dependent on the total volume of the storage facility $V_{storage}$ and the cost per volume of storage.

$$TAC_{storage} = EAC_{is} \cdot V_{is} + OPEX_{is} \quad (3.19)$$

The final part of the cost calculations is the transportation costs. The transportation costs are dependent on the transport distance $d_{i,j}$, and the mode of transportation which in turn depends on the transported good g . For example, the transportation costs for hydrogen are calculated using different parameters to the transportation costs for electricity, as they require different transportation infrastructures.

In general, the cost calculation for transportation is described by Equation 3.20. The transport costs are

directly proportional to the transport distance $d_{i,j}$ and the transport costs in terms of $[cost/distance]$. The binary variable $TN_{i,j,g}$ denotes the presence of transport infrastructure between echelons i and j for good g .

$$TAC_{transport} = TN_{i,j,g} \cdot d_{i,j} \cdot EAC_{transport,g} \quad (3.20)$$

3.2.2. Constraints

The constraints in the model can be grouped into balancing constraints, sizing constraints, and storage constraints. The balancing constraints start with electricity generation and hydrogen demand. Equation 3.21 balances the power generation by ensuring that the total electricity output $E_{ip,t}$ of all power generation plants is equal to the power input of all plants $E_{ij,t}$.

$$\sum_{I^p} E_{ip,t} = \sum_j \sum_I E_{ij,t} \quad \forall t \in T \quad (3.21)$$

Equation 3.22 denotes a similar balance for hydrogen production, where the amount of hydrogen produced in all electrolyzers $M_{ie,t}$ is equal to the amount of hydrogen sent from all electrolyzers to any other plant $M_{ije,t}$ for all timeslots $t \in T$.

$$\sum_{I^e} M_{ie,t} = \sum_j \sum_{I^e} M_{ije,t} \quad \forall t \in T \quad (3.22)$$

Equation 3.23 couples the mass and energy balance by relating the energy input and energy efficiency of the electrolyzer echelon to the amount of produced hydrogen. The amount of hydrogen produced is equal to the amount of energy entering the electrolyzer times the conversion efficiency η_{ie} of the electrolyzer. Since the balance of the electrolyzer must hold for all electrolyzers i^e , the sum of all hydrogen produced in all electrolyzers must also be equal to the total sum of hydrogen transported from all electrolyzers. This result, shown in Equation 3.24, is a general property of Equation 3.23 since if all individual plants are balanced, the sum of the individual plants is also balanced. In the rest of the model description, the overall balancing Equations analogous to Equation 3.24 will not be further defined.

$$M_{ie,t} = \sum_{j^e} E_{ije,t} \cdot \eta_{ie} \quad \forall t \in T, i \in I^e \quad (3.23)$$

$$\sum_{I^e} M_{ie,t} = \sum_{j^e} \sum_{i \in I} E_{ije,t} \cdot \eta_{ie} \quad \forall t \in T \quad (3.24)$$

Equation 3.25 shows demand balancing, where the sum of hydrogen $M_{ij^d,t}$ entering all demand sites j^d must be equal to the total demand D_t at time t respectively. From Equation 3.25 it follows that the total demand is the sum of the demands of each individual demand site.

$$D_{i^d,t} = \sum_I M_{ij^d,t} \quad \forall t \in T, i \in I^d \quad (3.25)$$

The final balancing constraint, Equation 3.26, ensures that the total amount of hydrogen entering demand from storage at any point in time is smaller or equal to the total amount of hydrogen in storage at that point in time. This ensures that in the model, hydrogen is not produced in one of the storage sites.

$$\sum_{j^d} M_{i^s,j^d,t} \leq M_{i^s,t} \quad \forall t \in T, i \in I^s \quad (3.26)$$

The next set of constraints presented is involved in system sizing. The first constraint, presented in Equation 3.27, correlates the size of the power plants with the amount of energy produced. Specifically, the amount of energy produced at all times in a single power plant is equal to the product of available irradiation, the combined size of that power plant, and the power plant efficiency, as shown in Equation 3.27.

$$E_{irr,t} \cdot n_{ip} \cdot \eta_{ip} = \sum_j E_{ip,j,t} \quad \forall t \in T, i \in I^p \quad (3.27)$$

In the model, the size of the electrolyzer is also directly coupled to the size of the power it receives, as no buffers are implemented between the two echelons to mitigate any intermittency. In Equation 3.28 this relation is shown, where the size of an individual electrolyzer is equal to the size of the maximum amount of electrical energy it receives times the efficiency of the electrolyzer. Note that this Equation does not hold for all $t \in T$ as it is only valid in the timeslot where the maximum amount of electrical energy is transported to the electrolyzer.

$$n_{ie} = \max_{t \in T} \left[\eta_i^e \sum_{I^p} E_{ip,j,t} \right] \quad \forall j \in J^e \quad (3.28)$$

Equation 3.29 relates the amount of electricity entering the electrolyzers and the amount of hydrogen leaving the electrolyzers through the electrolyzer efficiency.

$$\sum_j M_{i^e,j,t} = \sum_{I^p} E_{ip,j^e,t} \cdot \eta_{ie} \quad \forall t \in T, i \in I^e, j \in J^e \quad (3.29)$$

In Equation 3.30, the amount of water leaving all water treatment plants to a specific electrolysis plant i^e is based on the amount of hydrogen produced in that electrolysis plant and two conversion factors: γ_{LHV} , the lower heating value of energy stored in one unit of hydrogen and γ_{H_2O} , the mass of water required to produce one unit of hydrogen.

$$\sum_{I^w} M_{i^w,j^e,t} = M_{i^e,j,t} \cdot \gamma_{LHV} \cdot \gamma_{H_2O} \quad \forall t \in T, j \in J, j^e \in J^e \quad (3.30)$$

The size of the water treatment plant is determined based on the timeslot where the water production is highest. The required size of the water treatment plant is found through Equation 3.31. Inside the brackets, the total outflow of water from the water treatment plant to any other plant is multiplied by $\frac{1}{len(t)}$, which homogenizes the length of time. For example, if the timeslots used in the model are months, this ensures that the total amount of water produced in a month is corrected for the number of

days in the given month. After homogenization of the water production capacity, the minimal required size of the water treatment plant is found by finding the maximum value of water production in a single timeslot over all timeslots.

$$n_{iw} = \max_{t \in T} \left[\frac{1}{len(t)} \sum_j M_{iw,j,t} \right] \quad (3.31)$$

The following constraints, shown in Equations 3.32 to 3.35, determine the behavior of the hydrogen storage facility. Although strictly speaking, the size of the storage facility is bound by the physical size of the cavern and the operating pressure, the amount of hydrogen that is stored is still regulated in the model.

Equation 3.32 shows the balance of the amount of stored hydrogen within the storage facility i^s at a certain time $M_{i^s,t}$. The amount of stored hydrogen is equal to the amount of stored hydrogen in the previous time slot $M_{i^s,t-1}$, minus the amount of hydrogen that left the storage in the previous time slot $\sum_{j^d \in J^d} M_{i^s,j^d,t-1}$, plus the amount of hydrogen that enters the storage in the current timeslot $\sum_{i^e \in I^e} M_{i^e,j^s,t}$.

$$M_{i^s,t} = M_{i^s,t-1} - \sum_{j^d \in J^d} M_{i^s,j^d,t-1} + \sum_{i^e \in I^e} M_{i^e,j^s,t} \quad \forall t \in T, i \in I^s, j \in J^s \quad (3.32)$$

Equation 3.33, 3.34, and 3.35 define the initial storage value and the capacity boundaries of hydrogen storage.

$$\sum_{i^s \in I^s} M_{i^s,0} = M_0 \quad (3.33)$$

$$M_{i^s,t} \leq M_{i^s,max} \quad \forall t \in T, i^s \in I^s \quad (3.34)$$

$$M_{i^s,t} \geq M_{i^s,min} \quad \forall t \in T, i^s \in I^s \quad (3.35)$$

Various calculations within the model require the product of two model variables to be calculated. For example, to determine the total annual cost of transport $TAC_{transport}$ in Equation 3.20, the binary variable $TN_{i,j,g}$ is used to determine whether a transport connection exists between two echelon locations for a certain good g . In general, the multiplication of two model variables results in a non-linear representation of the model. For this purpose, the model makes use of linearization in order to reformulate the non-linear equations into linear equations. This is illustrated using the following example.

To calculate the total costs of transporting electricity, the binary variable $TN_{i,j}$ is multiplied with the distance $d_{i,j}$ (km) between the echelons, the cost of power infrastructure ($\$/TW/km$) and the required capacity of the powerlines n_i^p (TW) represented by the size of the solar plant. This results in a quadratic equation since both the binary variable and the size of the solar plant are considered variables in the model.

$$TAC_{transport,electricity} = TN_{i,j} \cdot d_{i,j} \cdot EAC_i^p \cdot n_i^p \quad (3.36)$$

To work around this problem, a new variable $VAR_{i,j}$ and constant M are introduced and the equation is reformulated as a series of inequality constraints.

$$M = Constant \quad (3.37)$$

$$VAR_{i,j} \leq M \cdot TN_{i,j} \quad (3.38)$$

$$VAR_{i,j} \leq n_i^p \quad (3.39)$$

$$VAR_{i,j} \geq n_i^p - M \cdot (1 - TN_{i,j}) \quad (3.40)$$

$$TAC_{transport,electricity} = VAR_{i,j} \cdot d_{i,j} \cdot EAC_i^p \quad (3.41)$$

In Equation 3.37 a constant is defined that is large enough such that $M \geq n_i^p$. Next in Equation 3.38 it is determined whether between connections i and j , the newly introduced variable $VAR_{i,j}$ is either 0 or a continuous variable where $0 < VAR_{i,j} \leq M$. Then in Equation 3.39 an inequality is introduced that ensures that $0 < VAR_{i,j} \leq n_i^p$. Finally in Equation 3.40 an inequality is introduced that ensures that $VAR_{i,j} = n_i^p$ when $TN_{i,j} = 1$ is 1 and $VAR_{i,j} = n_i^p - M$ when $TN_{i,j} = 0$. Essentially this series of inequalities combines the binary variable $TN_{i,j}$ and the size of the solar plant n_i^p into a single variable.

3.3. Performance indicators

Aside from the results provided by the model such as the total annual costs, mass and energy flows, and the sizes of the system component, additional metrics are used to analyze the performance of the system. In this section, these metrics are described and shortly elaborated.

As mentioned previously, the model minimizes the TAC of the system. Using the TAC allows for understanding the scale of the system as well as the number of required investments. However, a common way to represent the costs of hydrogen production is through the levelized cost of hydrogen (LCOH), a metric that shows the costs associated with producing one unit, commonly one kg of hydrogen. In order to more easily compare and intuitively understand the results of this work, the LCOH is used. The LCOH is calculated as the ratio between TAC (\$) and the amount of hydrogen produced (M_{H_2} , (kg)) as defined in Equation 3.42. Similarly for electricity generation, a common metric to use is the levelized cost of electricity (LCOE), as shown in Equation 3.43, as the ratio between the total cost of electricity production (TCE) and the total amount of produced electrical energy (E_{out}), expressed in cost per unit of energy.

$$LCOH = \frac{TAC}{M_{H_2}} \left(\frac{\$}{kg} \right) \quad (3.42)$$

$$LCOE = \frac{TCE}{E_{out}} \left(\frac{\$}{kWh} \right) \quad (3.43)$$

The LCOH and LCOE are cost metrics that are used to easily describe and compare the economic performance of the system. Next to the economic performance, the performance in terms of efficiency is also described. In this work, two main metrics are used to evaluate the efficiency of the system and compare them to other works. The first metric to describe the system efficiency is the overall system energy efficiency, which aims to provide an easy-to-understand metric for the energy losses within the system. In this work, the overall system energy efficiency is defined in Equation 3.44 below. In here η_{sys} represents the overall system efficiency as the product of the energy efficiency of individual system components η_i . The overall energy efficiency amounts to the fraction of the total amount of energy consumed in the demand sites $\sum_{j^d} M_{i,j,t}$ and the total amount of electricity produced in the solar plant $\sum_{j^p} E_{i,j,t}$.

$$\eta_{sys} = \prod_{i=0}^I \eta_i = \frac{\sum_{j^d} M_{i,j,t}}{\sum_{j^p} E_{i,j,t}} \quad (3.44)$$

The second metric used to evaluate the efficiency of the system is the capacity factor (CF), which shows the ratio between actual energy output versus theoretical maximum output and is defined according to Equation 3.45. The capacity factor can also be described more generally as the number of efficient hours of use of a technology. For example, the CF of an electrolyzer would describe the ratio between the amount of hydrogen produced versus the theoretical maximum amount of hydrogen that can be produced in that time, as shown in Equation 3.45. Similarly, for SWRO the CF shows the amount of water produced within a certain time compared to the maximum amount of water that can be produced in that time, as shown in Equation 3.46.

$$CF = \frac{E_{out}}{n \cdot t} \left(\frac{GWh}{GW \cdot h} \right) \quad (3.45)$$

$$CF_{SWRO} = \frac{V_{out}}{n_{SWRO} \cdot t} \left(\frac{m^3}{m^3/day \cdot day} \right) \quad (3.46)$$

There are various metrics that can be used to describe the performance of a system. A metric to describe the intensiveness of human intervention in nature is land use (LU). Land use shows how large a system is in terms of geographical area. Land use can be described as the amount of area required to build a certain technology. For example, for energy generation, LU would describe the area per installed capacity. To gain a better understanding of the scale of the system, land area for certain technologies will be calculated, according to Equation 3.47. In this equation, A denotes the total area (m^2) LU (m^2W^{-1}) denotes the land use intensity and n_i (W) is the capacity of a system component.

$$A = LU \cdot n_i \quad (3.47)$$

4

Case study

This chapter presents the case study used in the thesis to examine the hydrogen supply chain model presented in Section 3. First, a general description of the case study is given. Next, the system echelons are evaluated, extending on the decision-making process for the case study as well as going over the parameters used in the model.

4.1. Overview

In order to find the optimal design of a hydrogen supply chain and answer the main question of this work, a case study is selected and applied to the model described in Section 3. The case study considers a renewable hydrogen supply chain between Morocco, the Netherlands, and Poland. As discussed in Section 2.2, a renewable hydrogen supply chain consists of the following system echelons: Energy generation, Water purification, Electrolysis, and Energy storage.

For simplification of the case study, it is assumed that no part of the system infrastructure is currently present and the whole system must be built new. Taking into account the lifetime of the individual system components, this will give a fair overview of the expected production costs of hydrogen through the supply chain under consideration. In reality, this is not necessarily the case. For example, in Europe, a natural gas pipeline network already exists, that can be repurposed to transport hydrogen instead.

In Section 2.1 the geographical layout of the system and the echelon locations are already discussed. Table 4.1 shows the echelon coordinates as used in the model. Furthermore, this table presents the plant indices and approximate location of each echelon.

4.2. Input data and assumptions

The goal of the supply chain is to fulfill part of the hydrogen demand for the EU in 2050. Since the applied case study is over two decades in the future, assumptions about both the size and distribution of hydrogen demand are made. The demand assumptions made are in part based on the work of Smale, which is also part of the Pro2Tech project, and in part based on the Hydrogen roadmap Europe

Table 4.1: Echelon locations and parameters adopted in the model

Echelons	Index number i,j	Location	Coordinates (lat, lon)
Power	0	Marrakesh, Morocco	31.21,-7.35
Water	1	Essaouira, Morocco	31.79, -9.60
Electrolysis	2	Marrakesh, Morocco	31.63, -7.96
Storage	3	Groningen, Netherlands	53.30, 6.50
Demand 1	4	Assen, Netherlands	53.00, 6.58
Demand 2	5	Warsaw, Poland	52.27, 20.91

from the Fuel Cells and Hydrogen 2 Joint Undertaking as part of the EU [39, 71]. In the work of Smale, the hydrogen demand for the EU in 2050 is explored and three scenarios are substantiated. Two of the scenarios, named 'Realistic' and 'Average', are considered here.

The main difference between the two scenarios is the expected penetration rate of hydrogen in the energy mix. The 'Realistic' scenario considers hydrogen to play a significant role in transport, the decarbonization of industry as well as heating of buildings. In the 'Average' scenario, hydrogen is additionally used in the power production sector for the generation of electricity, resulting in a slightly higher hydrogen demand. The 'Realistic' scenario is expected to have an approximate hydrogen demand of 2200 TWh/yr, whereas the 'Average' scenario has an expected hydrogen demand of 2500 TWh/yr.

For the purpose of this case study, it is expected that the primary use of the hydrogen demand is to replace fossil-fuel use. Therefore it is assumed that hydrogen will be used mostly to cover the energy demand for heating and in the transport sector as well as the decarbonization of industry, as it is expected that the share of renewable electricity sources will increase in the coming decades. This assumption corresponds to the 'Realistic' scenario in the work of Smale, and coincides with the findings of the Hydrogen roadmap Europe. According to the Hydrogen roadmap Europe, to meet the requirements necessary for keeping the global temperature increase below 2 °C, an approximate amount of 2250 TWh/yr of hydrogen is required [71]. This amount would be able to provide for existing and new industry feedstock, heating and power demand for buildings, energy demand for transportation as well as power generation.

Although the work of Smale and the Fuel Cells and Hydrogen 2 Joint Undertaking come to a similar number regarding the hydrogen demand for the EU in 2050, the scenarios and penetration rate of hydrogen in the various sectors are different in both scenarios. For simplicity of the case study, in this work, a hydrogen demand of 2250 TWh/yr is assumed accordingly. This amount is not the demand required from the proposed supply chain in the case study, but rather the total final hydrogen demand for the whole of the EU. In order to increase energy security and avoid dependencies on a single region for the total of hydrogen supply, in this work it is assumed that only a part of the total demand can come from the proposed supply chain. For this reason, the case study assumes a hydrogen supply from the proposed supply chain of 780 TWh in a year. This figure corresponds to the Business-as-usual scenario in the Hydrogen roadmap Europe, and covers the supply of the minimum required hydrogen demand, corresponding to approximately 35% of the total expected hydrogen demand.

In the various scenarios, hydrogen would be required across the EU, mainly for industry, transportation, and power applications. However, it is outside of the scope of this work to accurately represent the spatial hydrogen demand requirements, therefore the distribution of hydrogen toward end-use applications is not taken into account. The demand of 780 TWh is distributed to two large demand sinks,

representing the east and west side of the EU.

The hydrogen demand for each demand sink must be fulfilled in every time slot, which requires a temporal demand pattern for hydrogen. In the case study, it is assumed that the monthly electricity demand pattern is a representative proxy for future hydrogen demand. Therefore, the hydrogen demand pattern for 2050 is estimated using the 2018 electricity demand pattern for the EU [72]. The year 2018 is chosen in order to mitigate the influence of the covid pandemic on the energy demand. The normalized demand pattern for the EU as used in the case study is shown in Figure 4.1.

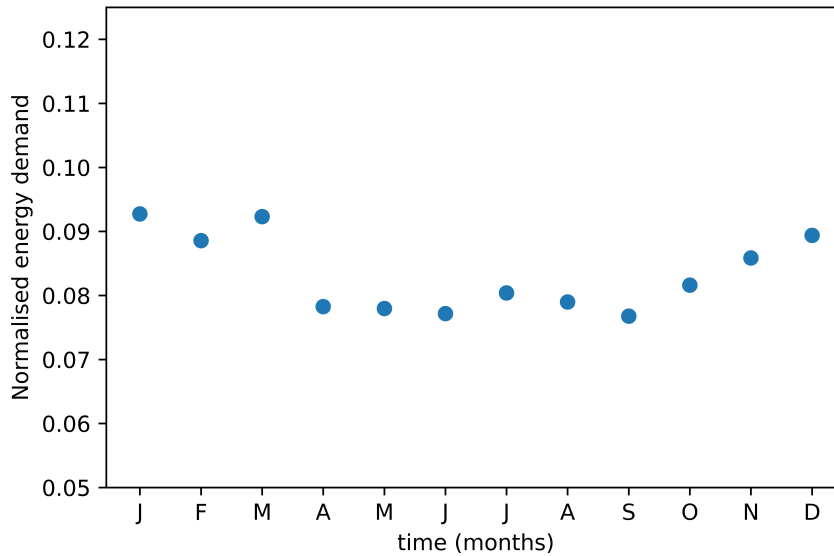


Figure 4.1: Normalised electricity demand for the European Union based on monthly electricity consumption. Original data retrieved from [72]

The available energy generation for the supply chain is based on solar irradiation at the location of the power plant. Irradiation data produced by NASA, represented as the mean solar irradiation ($\text{kWhm}^{-2}\text{day}^{-1}$) over the period of 2001 to 2020, is converted into monthly values, by multiplying the daily irradiation by the number of days in the respective month, and used in this case study [73]. The irradiation data in the model is expressed as peak solar hours per month and is shown in Figure 4.2. The peak solar hours represent the relative amount of hours that the solar panels operate under maximum capacity. Table 4.2 shows the capacity factor for each month based on the data used in the case study. The workflow of converting the raw data into the final numbers used in the optimization model is also represented in Figure 4.3.

4.2.1. Production technologies

This section will describe the assumptions and parameter values used in the model to describe the various echelons in the model. This section will explain the parameters that are used in the case study and the assumptions made to arrive at the parameter values.

In this case study, power generation is only available through PV panels. For these panels, it is assumed that they have a fixed orientation. As the research and development in the field of solar photovoltaics are still growing, assumptions about the costs and efficiencies of future PV systems must be made. In the irradiation data presented in Section 4.2, the efficiency of solar panels is already included. In order

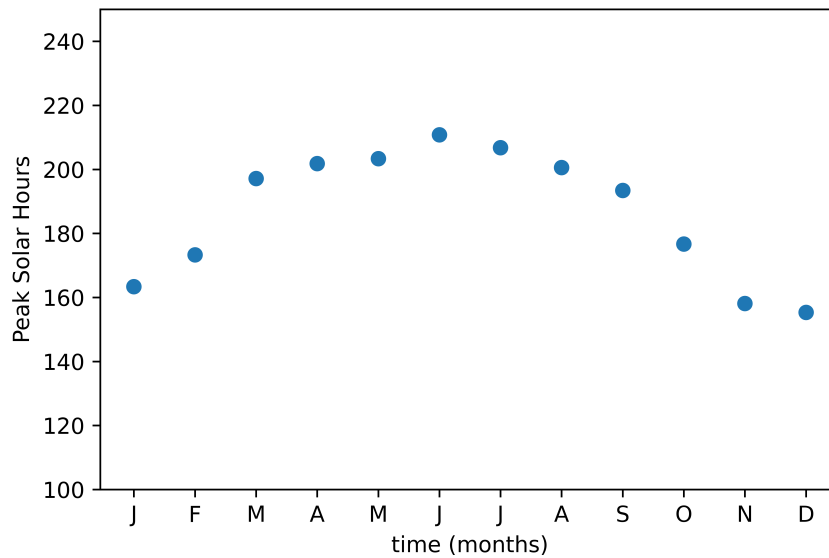


Figure 4.2: Scatterplot of the amount of peak solar hours equivalence of solar irradiation at the location of the power plant for every month in one year. Original data retrieved from [73]

to make an estimate for the price of solar panels in 2050, an overview of various cost predictions is made, as shown in Table 4.3. However, since methodologies for each of these studies differ, only the price estimates produced by IRENA are taken as model parameters for this work, in order to increase model consistency. After adjusting the currency of the cost estimates to 2020 USD, the price range of the PV system amounts to 170 to 495 $\text{\$}_{2020}\text{kW}^{-1}$. The average value of 333 $\text{\$}_{2020}\text{kW}^{-1}$ is used in the model as a base case price estimate for the PV system.

Similarly for electrolysis, multiple sources are consulted to find the average future cost prediction of alkaline electrolysis. The cost estimates are shown in table 4.4. In the case study, only the average price of the IRENA estimate is used, with a value of 219 $\text{\$}_{2020}\text{kW}^{-1}$. An assumption for OPEX of 2% of CAPEX per year is made.

The future costs of SWRO are adopted from Caldera and Breyer who used the cumulative installed capacity and learning rate to predict future RO costs [80]. After adjusting the currency to 2020 USD in order to maintain consistency, the projected CAPEX for SWRO amount to 632 - 1117 $\text{\$m}^{-3}\text{day}^{-1}$. For this work, the average of the two values, 875 $\text{\$m}^{-3}\text{day}^{-1}$ is assumed, corresponding to an average annual growth rate in SWRO capacity of 15%. Although in general the OPEX for SWRO is expressed in terms of the amount of volume produced, in this work 2% of CAPEX is assumed. This is because generally the electricity costs are included in the OPEX, however, in this work the electricity is produced within the supply chain itself. The sizing for the water purification system is determined by the amount of hydrogen required to be produced at a certain time. For each kg of hydrogen produced through electrolysis, approximately 18 liters of feed water is required, which is assumed to be entirely produced in the water desalination plant [81]. The desalination plant itself has an approximate energy requirement for water desalination using RO is approximately 5 kWh/m^3 water [48].

Table 4.2: Irradiation and solar PV capacity factor for every month as used in the case study. Original data retrieved from [73]

Month	Irradiation (peak solar hours)	Capacity factor
Januari	163	0.22
Februari	173	0.26
March	197	0.27
April	202	0.28
May	203	0.27
June	211	0.29
July	207	0.28
August	201	0.27
September	193	0.27
October	177	0.24
November	158	0.22
December	155	0.21
Average	187	0.26

Table 4.3: Overview of future cost estimations for PV systems

Reference	PV price estimate (\$/kW)
IRENA [74]	165 - 481
Pregger et al [75]	470
DNV GL [76]	431 - 689
Brändle [77]	266 - 434
Average	426

4.2.2. Transportation

In this case study, there is a need for transportation for electricity, water, and hydrogen. Electricity is assumed to be transported through high voltage alternating current (HVAC) powerlines. Costs for HVAC powerlines are adopted for 500 kV, single-circuit powerlines. The values presented are the average costs for 14 US states and the units are converted from $\$/\text{mile}^{-1}$ to $\$/\text{km}^{-1}$. The powerlines have an estimated maximum transfer capacity of 1500 MW per phase circuit [82].

Water and hydrogen are assumed to be transported through pipelines. The costs assumed for transportation infrastructure are presented in Table 4.5. The difference between the cost of pipelines for transporting water and hydrogen is explained through the assumption that in the EU a vast natural gas pipeline network is already present. Therefore, it is assumed that the pipeline costs for transporting hydrogen are slightly lower than for transporting water. In actuality, not the whole gas transport infrastructure required for this case study is present at the moment. Therefore, at locations where this infrastructure is absent as of now, the actual cost of hydrogen pipeline infrastructure is higher than presented here. The numbers presented in Table 4.5 are based on the amount of hydrogen or water transported through the infrastructure but do not take into account the capacity of the pipelines.

The transport costs are dependent on the distance of transport. As mentioned previously, the distance between echelons is determined as the direct line over the surface of a sphere between two points. The distances between echelons as used in the case study are shown in Table 4.6

4.2.3. Storage

In the model, only underground cavern storage for hydrogen is considered, located in Groningen, the Netherlands. The cavern storage suitable for hydrogen in Groningen is estimated to be able to store 31 TWh of working volume hydrogen [84]. However, in the case study, a value of 57 TWh is assumed, as

Table 4.4: Overview of future cost estimations for AEL systems

Reference	Electrolyser price estimate (\$/kW)
IRENA [78]	130 - 307
Roos [79]	171 - 598
Brändle [77]	200 - 450
Average	344

Table 4.5: Assumed costs for transportation infrastructure.

Transported good	Infrastrucutre	CAPEX	OPEX (% of CAPEX)	Lifetime
Electricity	Powerline	1.82 (M\$/km) [83]	5	50
Water	Pipeline	1.37 (\$/tpa/km) [77]	5	40
Hydrogen	Pipeline	1.08 (\$/tpa/km) [77]	5	40

the model is infeasible at a lower storage capacity. The costs associated with the storage of hydrogen in salt caverns assumed for this thesis is 297 €/MWh⁻¹, with an expected lifetime of 30 years [85]. The CAPEX value is converted to \$₂₀₂₀kWh⁻¹ resulting in a cost of cavern storage of 0.303 \$kWh⁻¹.

More recent insights into the storage of hydrogen in salt caverns, for example the work of Eradus, point towards a significantly reduced cost of storage compared to the number used in this work [86]. In the aforementioned work for example, it is estimated that the cost of hydrogen storage in salt caverns can be as low as 0.18 %kg⁻¹, which corresponds to a cost of 0.005 \$kWh⁻¹ using the LHV of hydrogen.

4.3. Cost parameters

This section aims to summarize the economic parameters used in the case study. In Table 4.7 an overview is given of the parameters presented previously in this chapter.

4.4. Assumptions

This section will give a short overview of the initial conditions assumed for the thesis. The first relevant initial condition is the starting month of the model. Since both supply and demand data show some form of seasonal variability, the operations of the model are dependent on the starting month. As shown in Figures 4.1 and 4.2, the amount of available energy production and the relative hydrogen demand shows a degree of anti-correlation. In this case study, the model is run starting from the first of January.

Since the case study starts at a point with relatively small energy availability and relatively high energy consumption, the case study adopts some initial storage at the start, corresponding to 50% of the working volume of the available cavern storage. This amount of initial storage is chosen to ensure that a sufficient volume of hydrogen is present during the starting months of the case study. To limit the impact of the initial storage on the overall model and case study outcome, another assumption regarding storage is that the amount of hydrogen stored after one year must be equal to or higher than the initial storage amount. By including this second assumption, the influence of the initial storage amount on the total amount of yearly production and sizing of the system is

Table 4.6: Distance (km) between echelon locations

Echelon (i)	Echelon (j)					
	1	2	3	4	5	6
1	0	223	75	2697	2671	3274
2	223	0	156	2718	2695	3353
3	75	156	0	2673	2648	3271
4	2697	2718	2673	0	33	974
5	2671	2695	2648	33	0	969
6	3274	3353	3271	974	969	0

Table 4.7: Overview of economic parameters for various technologies adopted for the case study

Technology	CAPEX	OPEX (% of CAPEX)	Lifetime
Production parameters			
Solar PV	333 (\$/kW)	2	25
Electrolysis	219 (\$/kW)	2	25
SWRO	875 (\$/m ³ /day)	2	10
Transportation parameters			
Powerline transport	1.82 (M\$/km)	5	50
Pipeline transport (water)	1.37 (\$/tpa/km)	5	40
Pipeline transport (hydrogen)	1.08 (\$/tpa/km)	5	40
Storage parameters			
Cavern storage	0.303 (\$/kWh)	2	30

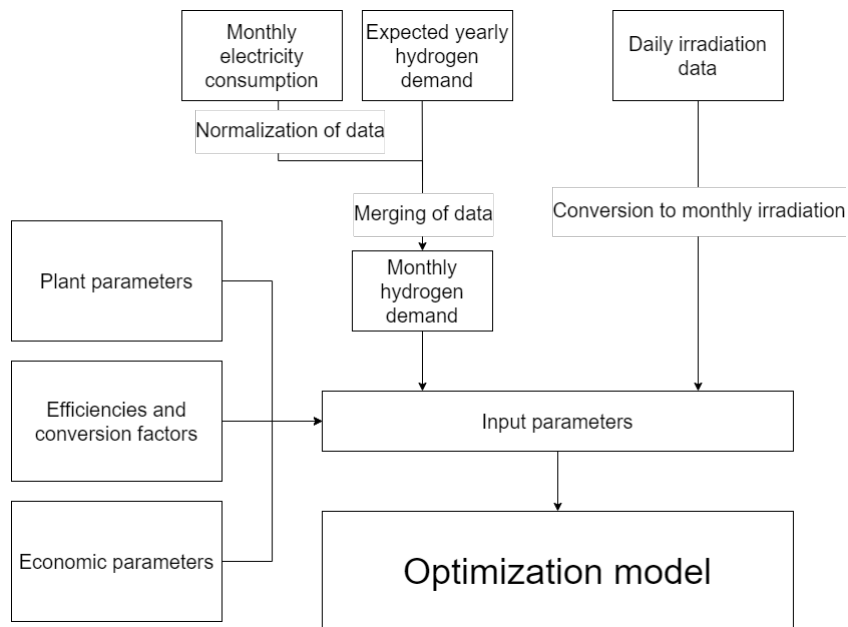


Figure 4.3: Schematic representation of the workflow of obtaining the input parameters that are used in the optimization model.

5

Results analysis

In this chapter, the results obtained from applying the case study to the mathematical model are presented. First, the results of the model in terms of system sizing, layout and transport strategy is discussed in Section 5.1. Secondly, the system operations are discussed in Section 5.2. Thirdly, the results of the economic performance are discussed in Section 5.3. Finally, the sensitivity analyses are presented and discussed in Section 5.4.

5.1. System sizing and transport strategy

The first results presented in this section aim to answer the research question of what the optimal size would be of a hydrogen supply chain producing renewable hydrogen. The echelons required for a hydrogen supply chain producing renewable hydrogen are already discussed in Section 2.2. In this section, the results of the model regarding the size of these echelons are discussed.

The first echelon is power generation, represented in the case study by solar PV. In order to produce 780 TWh of hydrogen to supply to the EU, the PV plant has a required size of 518 GW. Currently, the largest solar PV plant in the world has a capacity of 2.25 GW, making the solar plant in the case study 230 times larger [87]. The capacity factor is determined to be 0.256 and corresponds to the amount of peak solar irradiation presented in Section 4.2.

In addition, the size in terms of capacity for the solar plant, the size can also be expressed in terms of land use area required for this installation. According to NREL, the land use associated with fixed solar panels is 7.8 acres $\text{MW}_{\text{cap}}^{-1}$, or 31.57 $\text{km}^2\text{GW}_{\text{cap}}^{-1}$ [88]. This results in land use of 16,351 km^2 , corresponding to approximately 3.5% of the total area of Morocco. The size and land use parameters are also presented in Table 5.1

The next echelon is electrolysis, represented by AEL. The capacity of the electrolyzer is directly coupled to the capacity of the PV plant. Taking into account the efficiency, the size of the electrolyzer plant is determined as the energy entering the electrolyzer times the electrolyzer efficiency. This results in 347 GW of electrolyzer capacity. The capacity factor, measuring the efficient hours of operation in a year, is equal to 0.257, which is slightly higher than the capacity factor of the solar plant. This difference

in capacity factor can be explained by the fact that a small amount of energy is required for water treatment in the SWRO plant. The land use associated with the electrolyzer plant is $0.095 \text{ m}^2\text{kW}^{-1}$ installed capacity, resulting in a total land use of 0.2 km^2 [89].

The third and final plant for which the capacity is determined is the water treatment plant represented by SWRO. The capacity of the SWRO plant is directly dependent on the amount of hydrogen produced and is represented in terms of $\text{m}^3\text{day}^{-1}$. Since the time resolution of the model is monthly, a daily average of over a month is used to represent the SWRO plant capacity. In the model, the month that has the highest daily average hydrogen production is June, therefore the SWRO capacity is determined based on this outcome. In the case study, the highest SWRO capacity required is $1.31 \text{ Mm}^3\text{day}^{-1}$. In comparison, the world's largest SWRO plant has a capacity of $0,624 \text{ Mm}^3\text{day}^{-1}$, with a land use area of $100,000 \text{ m}^2$ [90].

Table 5.1: Size and land use for the PV, electrolyzer and SWRO plants.

System component	Component size	Land use (km^2)
PV plant	518 GW	16,351
Electrolysis plant	347 GW	0.2
SWRO plant	$1.31 \text{ Mm}^3\text{day}^{-1}$	33

The transport strategy of the system is concerned with the allocation of transport connections between echelons. In the case study, a connection is present between any echelon combination but is only used when there is a mass or energy flow between them. For electricity, the connections used are between the solar plant and electrolyzer as well as the water treatment plant. For water, the transport connection is used between the water treatment plant and the electrolyzer. Transport connections for hydrogen are used between the electrolyzer, storage, and both of the demand sites. From storage, there is only a connection in use to the demand site located in the Netherlands. The transport connections are summarized in Figure 5.1.

5.2. System operations

This section describes the results obtained for the case study associated with the system operations, including the mass and energy flows between system components. The system operations give a better understanding of how the system operates and what improvements can be made to the system.

Figure 5.2 shows the Sankey diagram associated with the energy flows of the optimal supply chain system. The flows in the diagram are given in units of TWh. The cyan vertical bar represents the electricity generation plant, which produces 1160.7 TWh of electricity in a full year. This energy is distributed to the electrolyzer (1158.6 TWh, blue) and water treatment (2.1 TWh, brown). In the electrolyzer, the electricity is converted into 780 TWh of hydrogen. This corresponds to the electrolyzer efficiency of 67% mentioned in Section 4. From the electrolyzer, 720.95 TWh of hydrogen is directly transported to one of the demand sites, 331.95 and 390 to demand sites 1 and 2 respectively. The remaining hydrogen with an energy content of 55.3 TWh is transported to storage first. From storage, 59.05 TWh of hydrogen is transported to the demand site located in the Netherlands.

The capacity factors for electricity generation, electrolysis, and water treatment are shown in Figure 5.3. As the electrolyzer is directly coupled to the electricity generation in the model, the capacity factors of both plants are nearly identical. There is a very slight difference between the two, as a small amount of electricity is used in the water treatment plant. The water treatment plant has an average capacity

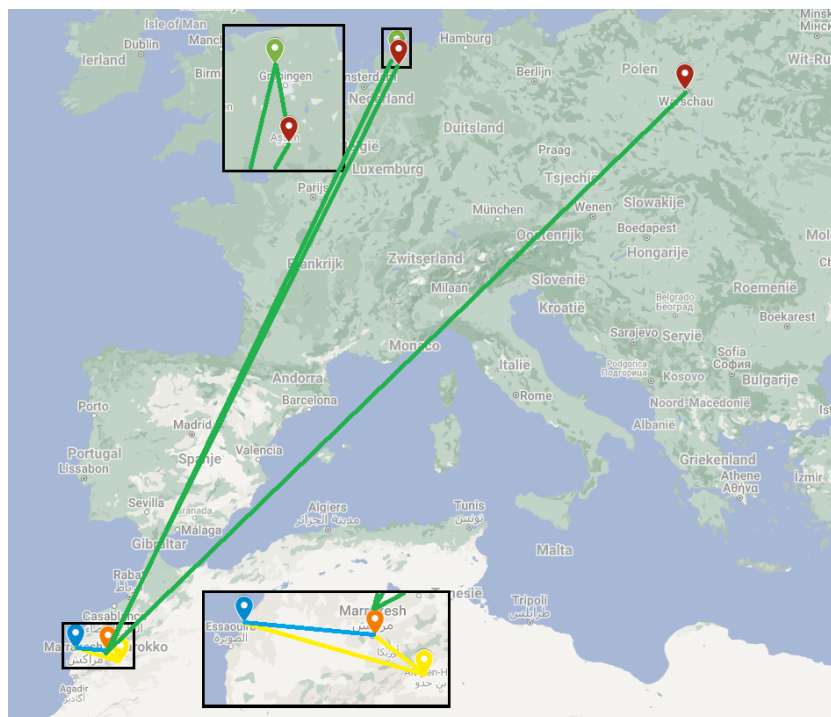


Figure 5.1: System layout of the supply chain model. Echelons presented are the solar plant (yellow), SWRO plant (blue), electrolysis (orange), hydrogen storage (green) and hydrogen demand (red). The lines between echelons indicate utilized transport connections. Transport connections utilized are for electricity (yellow, water (blue) and green (hydrogen).

factor of 0.87, where the capacity factor is lowest in December and highest in June. This corresponds to the months when the production of hydrogen is lowest and highest.

In figure 5.4 the monthly energy demand, hydrogen production, and storage amount are shown. The figure shows the seasonal behavior of hydrogen production and consumption and the resulting variability in the amount of stored hydrogen. At the start of the model in January, the production of hydrogen is lower than consumption, leading to the emptying of storage. For six months, from April until September, hydrogen production is higher than consumption, and storage is filled to 97 % of full capacity with the excess in production.

Although in the model storage is drained completely, realistically this should not happen as underground storage has a smaller operating range than 100% SOC. This constraint however is not implemented in the model. If this feature were implemented, this would require either the storage plant to be larger or the electricity generation and electrolysis plants to increase in size. It is expected that increasing the size of the storage facility will be the lowest cost solution, as the sensitivity of the TAC to storage is small, which will be explained in Section 5.4.

Although the storage site selected for this case study is expected to have a working volume of 31 TWh of hydrogen, the minimum amount of storage required is 57 TWh. Lowering the storage amount creates an infeasible problem. Increasing the available storage amount does not influence the optimal system sizes, mass, or energy flows.

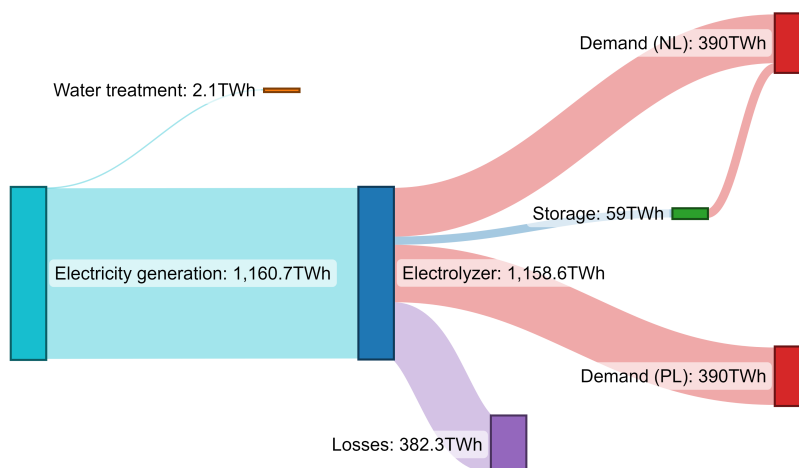


Figure 5.2: Sankey diagram of energy flows of the optimized supply chain.

5.3. System costs

This section provides an overview of the costs of hydrogen production in the supply chain of the case study. For all calculations, an interest rate of 7% is assumed.

In order for the model to be optimized, the total annual costs are minimized. For the optimized model, these costs equate to 36.55 B\$ per year. This number takes into account the lifetime of all system components and therefore includes the replacement of system components. The cost for one kilogram of hydrogen (LHV 33,33 kWhkg⁻¹) to be produced and transported to one of the demand sites is 1.56 \$kg⁻¹. This corresponds to a cost per unit of energy of 0.047 \$kWh⁻¹ for hydrogen. In the model, the costs of electricity production from the PV plant are 0.023 \$kWh⁻¹ (0.78 \$kg⁻¹) and therefore amount to approximately half of the overall final hydrogen costs. The cost contribution of the other echelons are 0.34 \$kg⁻¹ (22%) for electrolysis, 7.68*10⁻⁵ \$kg⁻¹ (0%) for water treatment using SWRO, 0.40 \$kg⁻¹ (26%) for transport and 0.037 \$kg⁻¹ (2%) for hydrogen storage. A full cost breakdown of the LCOH is presented in figure 5.5.

The results of the breakdown of LCOH of this work are compared with the works of Doodeman and Roobeek, who have performed similar analyses [24, 25]. In the work of Roobeek, a green hydrogen supply chain using only solar PV between Oman and the port of Rotterdam was assessed. In the work of Doodeman, green ammonia production in Morocco is assessed. The trends over all these works show that electricity production costs amount to approximately half of the overall costs and electrolyzer costs amount to approximately a quarter of LCOH. Both the work of Roobeek and this work find that transport costs amount to approximately 25% of LCOH. In all works, water feedstock costs are negli-

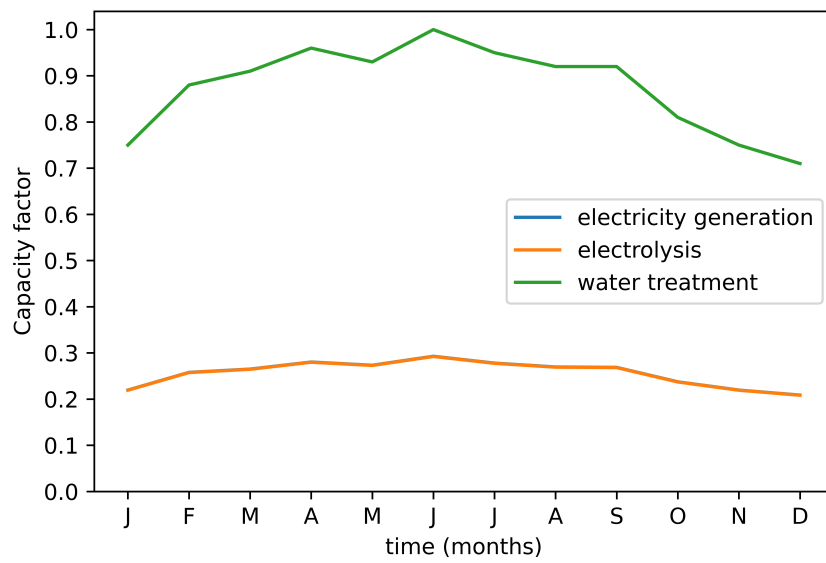


Figure 5.3: Capacity factors of the electricity generation, electrolysis, and water treatment plants throughout the year.

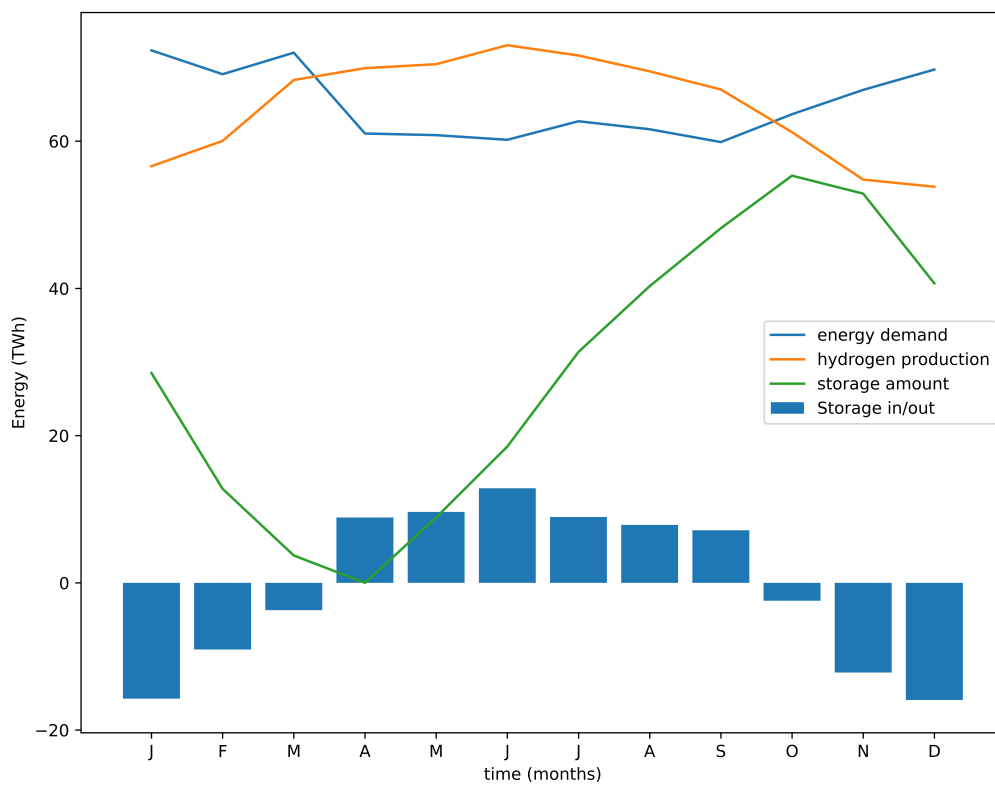


Figure 5.4: Overview of monthly hydrogen demand, hydrogen production, storage amount, and storage in- and outflow.

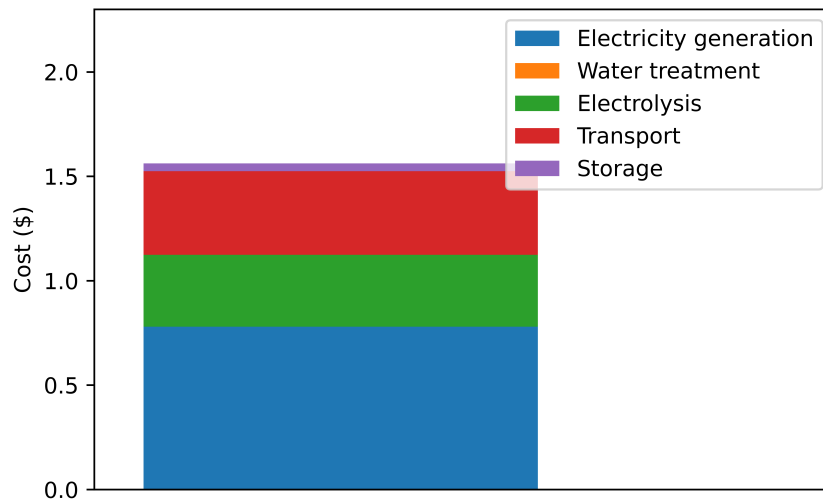


Figure 5.5: Cost breakdown of the LCOH of hydrogen in the proposed supply chain and case study

gible compared to all other costs.

One significant difference between the works of Roobeek and Doodeman compared to this work is the absolute cost predictions. In this work, the prediction of overall costs is approximately 25% lower compared to Roobeek, and about 5% lower compared to Doodeman. Due to the comparable cost contributions of the system components across works, it is expected that the variance in absolute cost predictions can be explained on the basis of economic parameters introduced in the modeling, rather than the models of the system themselves.

Comparing the economic parameters across works, some anomalies can be pointed out. First, the overall energy efficiency of the full system is lower in the work of Roobeek. Even though the economic parameters used for the PV system ($321 \text{ \$kWp}^{-1}$) and electrolyzer ($200 \text{ \$kW}^{-1}$) are comparable to the ones used in this work, the difference in energy efficiency accounts for approximately half of the price difference. Another contribution to the price difference between these works is the overall efficiency or capacity factor of the solar plant and in extension the electrolyzer. In the work of Roobeek, an average energy output of 4.56 GWh/day/GW for the PV system is reported. In this work, the efficiency of the solar plant is higher at 6.14 GWh/day/GW. These factors alone contribute to a price difference of nearly 25% across the supply chain.

Comparing the economic performance of this work with the work of Doodeman provides an additional challenge, as the results of the work are published in euros rather than dollars. However, at the time of publication of this document, the exchange rate is approximately 1.00 EUR/USD. The economic parameters used in the work of Doodeman for the PV system are 400 €/kWp and 180 €/kW for the electrolyzer, compared to 333 \$/kWp for PV and 219 \$/kW for electrolysis. As electrolysis contributes almost double the costs of PV in the model, the larger electrolyzer costs weigh more heavily than the lower PV costs. At the mentioned exchange rate, this difference in economic parameters covers the full price difference between this work and the work of Doodeman. If the economic parameters of Doodeman are adopted in the model of this work, the LCOH equates to $1.66 \text{ \$kg}^{-1}$.

Table 5.2: Cost breakdown comparison of LCOH

Cost contribution (%)	This work	Roobeek [25]	Doodeman [24]
Total cost (\$/kg)	1.56	2.17	1.63 (euro/kg)
PV	49.9	49.4	49.8
electrolyzer	22.0	22.8	28.4
Water	0.005	0.5	0.23
Transport	25.7	22.6	-
Storage	2.3	1.5	-
Other	0	3.2	21.57

5.4. Sensitivity analysis

In this section the sensitivities of the model are analyzed. For all sensitivity calculations, all variables are constant except the variable under consideration. Since the model attempts to find the costs of a future supply chain, the cost parameters are uncertain. In order to see the effects of the possible variance of technology costs, a sensitivity analysis is performed.

5.4.1. Technology costs

For the technologies where cost ranges are given, the analysis is performed on the full cost range. For example, the cost of a PV system is estimated between 170 and 495 \$kWp⁻¹, therefore the sensitivity analysis is performed with these values as extremes. For technologies without a clear cost range estimate, a value of 30% is taken.

The sensitivity analysis starts with an overview of the influence of the cost range estimates on the total annual costs for each technology used within the model. The results of this analysis are shown in Figure 5.6. The results of the sensitivity analysis are in accordance with the cost contributions of the echelons described in Section 5.3. The largest sensitivity is found in the cost for electricity generation, followed by electrolysis and hydrogen pipelines.

The cumulative sensitivity of the system results in a cost range for the TAC of 21.2 - 51.6 B\$, corresponding to a LCOH of 0.91 - 2.21 \$kg_{H₂}⁻¹. The cost ranges resulting from the sensitivity analysis are in descending order 17.8 B\$ (59%) for electricity generation, 6.5 B\$ (21%) for electrolysis, 5.6 B\$ (18%) for hydrogen pipelines, 0.47 B\$ (2%) for hydrogen storage, 0.02 B\$ (<0.1%) for powerlines and water pipelines and 0.001 B\$ (<0.1%) for water treatment. The results indicate that even with uncertainty in future prices, the resulting LCOH from this supply chain will likely be between 1 \$kg_{H₂}⁻¹ and 2 \$kg_{H₂}⁻¹, where the price of electricity generation has the most significant influence on the final costs.

5.4.2. Interest rate

The results of the model in terms of projected costs are not only dependent on the technology costs. As shown in Equation 3.12 and 3.13 in Section 3, the projected TAC depends on both the technology cost as well as the interest rate. In general, the interest rate of a loan for a large investment depends on the risk associated with the investment. A higher risk results in a higher interest rate, as the return on investment, is less certain. For this project, an interest rate of 7% is assumed for all investments. However, as the lifetime of certain plants within the system can be large, for example, a projected technology lifetime of 50 years for powerlines, the interest rate can have a large influence on the projected TAC.

In order to determine the impact of the interest rate on the TAC, a sensitivity analysis for the interest

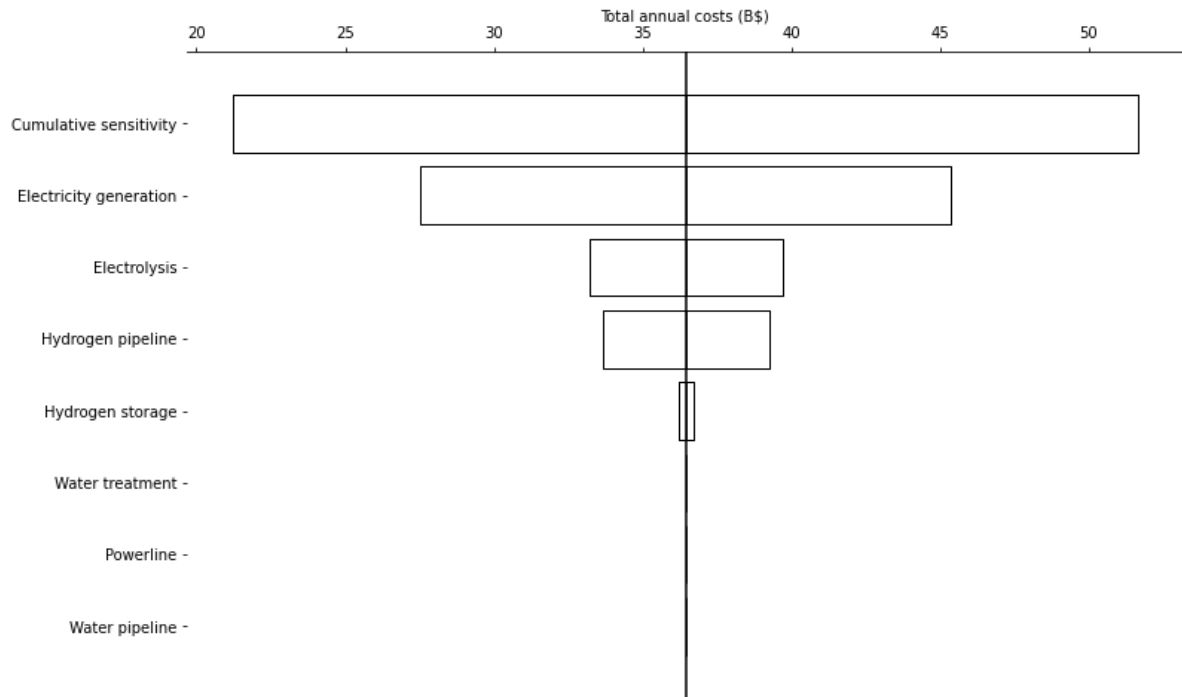


Figure 5.6: Tornado plot of the performed sensitivity analysis. The plot shows the cost ranges for the overall system as a result of price uncertainty for the various technologies.

rate is performed. The results of the analysis are shown in Figure 5.7. The analysis of the interest rate, ranging from 0 to 10%, shows that the range of TAC varies between 19.8 - 44.9 B\$, corresponding to a LCOH of 0.846 - 1.92 \$kg_{H₂}⁻¹. At 0% interest rate, the TAC are 46% lower than the base case and at 10% interest rate the TAC are 23% higher than the base case at an interest rate of 7%. This indicates that the interest rate is a significant factor on the overall project costs. In fact, the calculated range of TAC with varying interest rate is higher than any of the individual technologies.

5.4.3. Initial conditions

For the model to run, some initial conditions must be set. The initial conditions are the amount of hydrogen initially stored and the starting month of the model. Changing these initial conditions influence the outcome of the model. The degree to which the initial conditions determine the system costs are presented in this subsection.

Another initial condition that is investigated is the initial storage amount. For the initial storage amount, any amount below 49% of maximum storage capacity results in an infeasible problem. Above an initial storage value of 70% of maximum capacity, the model is also infeasible. When the initial capacity of storage increases, the echelon sizing of the PV plant and electrolyzer plant decrease. This effect is shown in Table 5.3. From this table it can be seen that improvements for the optimal plant sizes are made with a change in initial storage, however, this effect is relatively small. Initial storage values higher than 60% of maximum storage capacity do not result in a change in optimal plant sizes. The effects are likely due to the condition in the model that ensures that the amount of stored hydrogen in December is higher or equal to the amount stored in January of that year. In the case study, however, 3.8 TWh more hydrogen leaves storage than is put back in during the time window. This is because the value of the storage amount is taken at the start of the month, however, during the month hydrogen

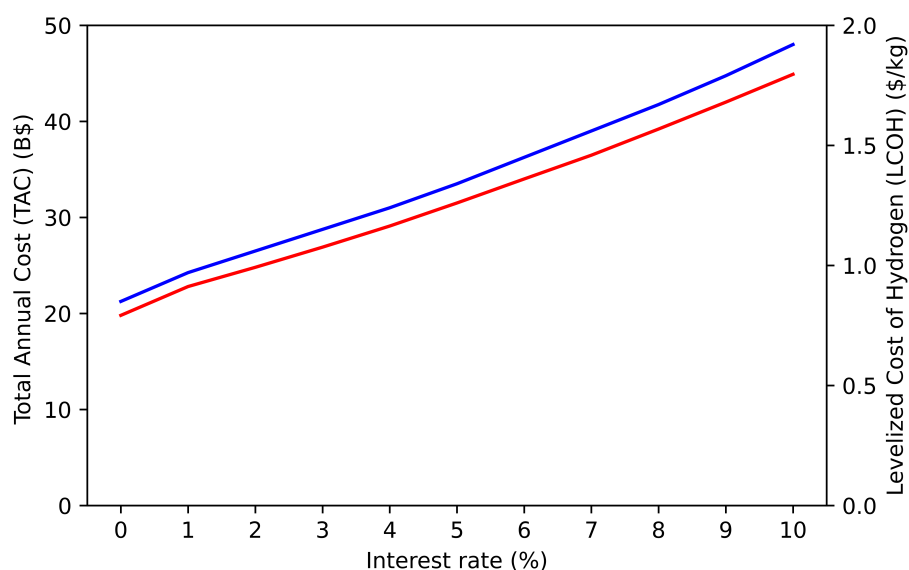


Figure 5.7: Sensitivity of the model to the interest rate. Interest rate ranges from 0% to 10%. The general model assumes a value of 7%. The sensitivity is shown to both the TAC (red) and LCOH (blue).

can still leave. Since December has a high energy demand from storage, this results in a mismatch. A longer time window for the case study would solve this issue.

Table 5.3: Effect of initial storage on the optimal size of the PV, electrolyzer and water treatment plants.

Initial storage %	50	55	60	65	70
Initial storage (TWh)	28.5	31.35	34.2	37.05	39.9
PV (GW)	518	510	509	509	509
electrolyzer (GW)	347	341	341	341	341
Water treatment (Mm ³ /day)	1.31	1.25	1.25	1.25	1.25

The starting month for the model is set to Januari as a default value, for which the model is then run for a full year. Although the starting month should not change the model outcome, due to the storage constraints, a slight variation in system size is measured when the starting month is changed. As mentioned previously, the model takes the final value of storage at the start of the month, however during the month this hydrogen can still leave storage, resulting in a mismatch. As a result, when the model starts in a month where supply is larger than demand, the system will be oversized compared to the base case, since the amount of hydrogen that must be produced during these months is slightly higher. The results of this analysis are presented in Table 5.4. Interestingly, when the starting month is set to one of the final four months in the year, the model becomes infeasible. The reason for the infeasibility is not investigated further.

5.5. Discussion of results

5.5.1. Cost comparison to alternative supply chains

In order to put the results related to system costs into perspective, a comparison is made between this system and alternative hydrogen sources. In this analysis, three main production technologies, electrolysis, steam methane reforming (SMR) and coal gassification (CG), are compared based on

Table 5.4: Results of sensitivity to the starting month of the model. Inf indicates the starting month results in an infeasible problem

Starting month	TAC (B\$)	LCOH ($\$/kg_{H_2}$)	PV size (GW)	electrolyzer size (GW)
Januari	36.55	1.56	518	347
Februari	36.09	1.54	511	343
March	36.26	1.55	514	344
April	36.65	1.57	520	348
May	36.73	1.57	521	349
June	36.76	1.57	521	349
July	36.89	1.58	523	351
August	37.09	1.59	523	352
September	inf			
October	inf			
November	inf			
December	inf			

their LCOH. As one of the goals of a renewable hydrogen supply chain is to reduce GHG emissions for energy generation, the costs for SMR and CG include the use of carbon capture and storage (CCS) technologies. An overview of the comparison is presented in Table 5.5.

The cost range of low-carbon hydrogen production for alternative hydrogen sources ranges between 1.66 - 2.79 $\$/kg_{H_2}^{-1}$. The methods used across the research to obtain the values differs, and therefore this is not a perfect comparison. An in-depth analysis of the methodologies of each study is not performed. The resulting costs from this work are on the low side compared to alternative hydrogen sources, but still plausible.

Table 5.5: Cost comparison table of various low carbon hydrogen production methods. The compared technologies are Steam Methane Reforming (SMR), Coal Gassification (CG) and electrolysis. For GC and SMR, the cost of CCS is included.

Source	Generation technology	Hydrogen cost ($\$/kg$)
This work	Electrolysis	1.56
CSIRO [91]	Electrolysis	1.86
NREL [92]	Electrolysis	2.64
IEA [89]	Electrolysis	2.39
IRENA [93]	Electrolysis	2.06
BNEF [94]	Electrolysis	1.66
Salkuyeh et al. [95]	SMR	2.33
IEAGHG [96]	SMR	1.98
CE Delft [97]	SMR	1.98
IEA [89]	SMR	2.22
BNEF [94]	SMR	2.79
IEAGHG [98]	CG	2.74
CSIRO [91]	CG	1.88
IEA [99]	CG	2.13
BNEF [94]	CG	2.23

The techno-economic parameters used in the case study are all assumed, therefore there is a large variance in the actual LCOH. However, based on the sensitivity analysis presented in Section 5.4, it is expected that the costs of this system will not exceed the projected costs of the alternative systems described in Table 5.5. Furthermore, the electrolyzer capacity factor is directly coupled to the PV capacity factor, resulting in oversizing of the electrolyzer plant and an increase in electrolyzer costs. It is expected that the costs can be reduced by including additional renewable energy technologies, for example, wind, alongside solar as it is shown that these have some degree of anti-correlation, leading

to an increase in the capacity factor of the electrolyzer.

There are also factors that could lead to an increase in the costs of the proposed supply chain. Distribution of hydrogen to end-use requires a larger transport infrastructure than considered in this work, which could lead to a significant increase in transportation costs. Furthermore, short-term fluctuations in renewable energy availability are not taken into consideration as the system is modelled on a monthly timescale. The effect of short-term intermittency on the performance of the system is not considered for this work.

The electrolysis plant is expected to be oversized by the model. Due to the absence of electricity storage options between the PV plant and the electrolysis plant, the electrolyzer is expected to work intermittently, resulting in a capacity factor of approximately 0.256. Realistically, the capacity factor of the electrolyzer plant should be as high as possible to reduce electrolyzer size and in turn capital investment.

6

Discussion and recommendations

This chapter provides a discussion of the work performed for this thesis. First, the main findings of this work are discussed. Next, the limitations of the model developed for this work, followed by the limitations of the case study are addressed. Finally, recommendations for future work are presented.

6.1. Main findings

As stated in the introduction, this work is exploratory research with a focus on finding the factors that impact the economic performance of a large-scale international renewable hydrogen supply chain. Through the use of a case study that is applied to an optimization model, some of these factors have been identified and presented in Section 5.

One of the concerns for establishing a hydrogen supply chain specifically between Northern-Africa and the EU is water scarcity. In order to negate the effect of water scarcity, the case study includes the production of the water supply required for electrolysis through SWRO. Based on the results of this work, including seawater purification as an integral part of the supply chain is a viable way of securing water supply. The costs associated with the purification of seawater are negligible compared to the overall system costs. Moreover, the required size of the purification plant is only twice the size of the largest plant in existence today, indicating little to no technical limitations for the technology itself.

In contrast to the limited economic impact of integrating the water supply, the impact of transportation on economic viability is high. In this case study, transportation is the second-highest cost contributor to the overall system. This is partly due to the relatively high cost of transport infrastructure, but mostly due to the large transport distance for hydrogen. Despite transportation already being the second highest cost contributor, it is expected that the share of transportation costs will be higher with a more adequate description of the system. In this work, several assumptions, that limit the cost of transportation, are made to simplify the representation of the transportation network. Firstly, the maximum capacity of a transport connection is not taken into account within the model, resulting in no additional costs for high-load transport networks. Secondly, it is assumed in the model that hydrogen infrastructure is repurposed from natural gas infrastructure, reducing capital costs. Although a vast natural gas network is present in the EU it does not span the overall system assumed in this work [100]. Not only main

transport infrastructure is partly insufficient, but also connections between system components, for example, storage and demand sites, and the main infrastructural routes are not present currently.

Another finding of this work concerning the network of the supply chain infrastructure relates to the storage of hydrogen. As shown in Figure 5.1, the only connection utilized that is leaving storage is towards the demand site in the Netherlands. Although storage is required to mitigate the seasonal mismatch between hydrogen production and consumption, it indicates that only part of the system has to be balanced using large-scale storage in order to mitigate the seasonal effect for the overall system. Since a base load of hydrogen production is present at all times of the year, the capacity of seasonal storage can be relatively small. In this case study, the working storage capacity is approximately 7.5% of the total yearly demand.

The final point about the supply chain system concerns the results on the land use area required for the operation of the system. One of the more concerning results regarding the viability of the proposed system is the land use associated with electricity generation. As the size required for the solar plant is 230 times larger than the current largest installed solar plant, it is reasonable to assume that it is not viable to have a single solar plant produce all the required electricity for the system. Rather, based on the results of this work it is expected that a more decentralized system of multiple smaller electricity generation plants is more realistic. Besides, in the case study in this work, only solar PV is considered as electricity generation technology, whereas in practice, a combination of multiple different renewable electricity generation technologies is favorable. The implications of a more decentralized electricity generation system on the layout and operations of the overall network are not investigated in this work. It is clear that an increase in the decentralization of electricity generation plants also results in an increase in network complexity. In turn, this may also lead to the need for multiple water purification and electrolysis sites, which would require more suitable locations. The full extent of this effect is not investigated, as it is outside the scope of this research, however, it needs to be addressed as the representation of the system and the network within this case study is an oversimplification of the real-world implementation of this system.

6.2. Model limitations

The model created for this work contains all vital echelons required for a renewable hydrogen supply chain. It produces green electricity, uses this electricity to produce fossil-free hydrogen, and transports and stores this hydrogen over longer timescales. Moreover, in the model the water feedstock is created within the system itself, eliminating competition over clean water. The first major limitation of the model is that energy losses in the system are not fully represented. Transport and storage losses as a result of powerline transportation, boil-off of hydrogen, energy use for compression, and other mechanical parts are not taken into account. The only energy losses present in the model are those of the electrolyzer.

The next major limitation is that the supply chain represented by the model is a closed system. Although the proposed supply chain may in principle be created as a closed system, it is safe to assume that there will be interaction with the supply chain from actors outside of the system. For example, if the PV plant would not only provide power for the supply chain in this model but also for domestic or other industrial purposes, this would most likely have an impact on the sizing, operation, and costs of the proposed supply chain. Furthermore, as water scarcity is becoming a larger problem, it can be reasonably assumed that if a water treatment plant is built to provide clean water for energy production, this would come into conflict with local populations who may need the same resources. The extent to which

these factors influence the model outcome is unknown, and arguably impossible to fully encompass in the model.

The inability to store electricity or water in the model is another major limitation, that impacts the performance of the overall system. Since electricity cannot be stored between the energy generation and electrolysis echelons, the capacity factors of both echelons are coupled. Electrolysis can only be performed when the power plant is generating power. This results in over-sizing of the electrolysis plant as well as a lot of losses in real-world applications due to constantly switching on and off. It is expected however that implementing more storage options throughout the supply chain will positively influence the performance of the model.

Finally, the model is a single objective multi-period model to minimize the TAC. However, the real-world application of the modelled system in this work would be to produce hydrogen in order to reduce fossil fuel use and in turn GHG emissions. Therefore, a logical step for the model would be implementing GHG emissions tracking. This would allow the comparison between fossil-fuel-based energy systems and the modelled energy system. Furthermore, the model could be transformed into a multi-objective optimization model where minimizing GHG emissions would be an additional objective.

6.3. Case study limitations

The case study itself also has some limitations. One of the main limitations is the way time is handled in the model. First, the scale of operations is only a single year, which could influence the model results. If more years are modelled, this could influence the decision-making of the model on the system sizing as well as storage behaviour. Furthermore, the time resolution of a monthly scale in the case study ignores a lot of factors that may influence the system. For example, using an hourly scale would result in a much better representation of intermittency of renewable energy production, for example by including days of consecutive low irradiation. This would also have an effect on the sizing and operation of the system.

Since the case study assumes the supply chain to exist in 2050, 28 years from now, a lot of assumptions about the techno-economic parameters, for example, electrolyzer efficiencies or future technology costs, are made. However, the market for renewable energy technologies can be very volatile and rapid acceleration or stagnation in technology improvements is not rare. This work attempts to include the development in techno-economic parameters while keeping the assumptions realistic. Moreover, price reductions through system scaling are not taken into account. However, it can be reasonably assumed that an increase in system size will lead to relative cost reductions. For this work, it is assumed that the scale of the system is sufficiently large that further cost reductions related to system scaling are not present.

Another factor influencing the model and case study performance is the limited amount of technologies implemented. Although the supply chain under consideration is able to provide renewable hydrogen, there are alternative technologies available that are not explored. Renewable power can be generated using wind, or a combination of both solar and wind. Furthermore, the solar panels assumed in the case study have a fixed layout, however, PV systems with single or double-axis tracking do exist and are more efficient, but also more expensive.

The same holds for electrolysis, where a combination of multiple technologies is arguably preferred on the scale that is represented in the case study. SOEL is very efficient compared to AEL and PEM, how-

ever, is not able to run intermittently. PEM has a fast start-up time compared to AEL and is, therefore, better suited for intermittent energy supply. Although the time scale of the model does not take into account ramping and start-up of the plants, in a real-world application, this would need to be addressed. For example, SOEL can be used for base load, AEL for medium-term fluctuations (hours-days) and PEM for short-term fluctuations (minutes-hours). This would arguably lead to a more efficient system and as a result a lower system size.

For transport, it is assumed that transportation of power and water over short distances (<250 km) is the most cost-effective using HVAC powerlines and pipelines respectively. Intercontinental transport of hydrogen however may be more economically attractive using for example shipping, depending on the location of the demand sinks.

This leads to the next limitation, which is the existence of only two demand sinks. In a realistic scenario, the hydrogen demand for the EU would need to be transported and distributed throughout the EU as well. It is expected that a large share of the transport infrastructure cost comes from the distribution of hydrogen from hubs to the end-use destination. Since the generation of hydrogen is centralized in this case study, this would imply adding much more demand sinks throughout the EU to make the transport costs more realistic.

6.4. Recommendations

The main goal of this work was to gain a better understanding of a large-scale hydrogen supply chain between northern Africa and the EU. As exploratory research, this has been successful. Nevertheless, improvements to the model and case study can be made that would improve the quality of this work. In this section, three recommendations are given for future research, that can be directly applied to improve this work, but also to aid in the approach of similar future works.

Rescoping the model objective. In this work, producing low-carbon hydrogen is achieved by including low-carbon, renewable technologies such as solar power combined with electrolysis. To gain a better understanding of the environmental impact of a renewable hydrogen supply chain, this impact in terms of emissions should be explicitly included in the model. As a first approach, this can be done by tracking the overall emissions produced in the system. For a more in-depth analysis, the problem can be formulated as a multi-objective optimization problem, where emissions are part of the decision-making for optimizing the system.

Additions to the model. Several additions to the optimization model can be made to improve the realism of the results. First, energy losses within the system should be taken into account. Second, storage options for water and electricity between water treatment and electricity generation respectively and electrolysis can be included in the model. This will likely reduce over-sizing of the electrolysis and water plants as they will not be directly coupled to the output of the electricity generation plant. Finally, adding sinks for water and electricity to cater to the needs of local populations is greatly encouraged, as this would create a more fair design of the system for all involved stakeholders.

Additions to the case study. As mentioned, one of the main limitations of the case study is the way time is handled in the model. By increasing the time resolution of the case study, the effect of short and medium-term intermittency of electricity can be included in the model outcome. Extending the time span of the case study to multiple years is also expected to influence the decision-making of storage behavior, and will enable the incorporation of yearly variability in energy supply and demand.

Furthermore, in order to avoid so-called lock-in situations and give a fair chance to develop technologies, alternative technologies can be implemented alongside proven technologies. For technologies that are included in the case study, multiple variations can be included. For example, next to electricity generation, wind and geothermal energy could be incorporated, in order to investigate whether the use of multiple technologies alongside each other would influence the overall viability of the proposed system.

Finally, a more elaborate transport and distribution network can be modeled and included in the case study. In this work, transport amounts to approximately 25% of the overall costs. This transport network however only supplies two locations within the EU, implying that transportation costs will be a bigger fraction of total costs when the number of demand sites increases. Moreover, a more thoughtful design of the transportation network may be valuable, for example by introducing transport nodes where transport connections are allowed to branch off. This would eliminate the placement of multiple transport connections along the same route.

7

Conclusion

The goal of this work is to gain a better understanding of the economic performance of large-scale green hydrogen production with a focus on finding the optimal supply chain layout and operations of an international supply chain between northern Africa and the European Union. A literature analysis is performed in order to evaluate the required system echelons as well as the technologies that can act as system components for the echelons. This evaluation led to the conceptual design of the supply chain which includes electricity generation by means of solar PV, water treatment using SWRO, alkaline electrolysis, hydrogen transport through pipelines, and underground hydrogen storage in salt caverns.

To find the sizes of system components and the economic performance of this system, an optimization-based cost model is set up. The model describes the operation of a hydrogen supply chain and determines the optimal size of the system components as well as the mass and energy between system echelons over a time range. The cost model takes into account the CAPEX, OPEX, and lifetime of the system components to arrive at the total annual costs of the overall supply chain.

This model was then applied using a case study to determine the optimal supply chain configuration and the economic performance of this optimized supply chain. Using the case study described in this work, the model found an annual cost of the supply chain of B\$ 46.37 providing 780 TWh of renewable hydrogen to the EU, corresponding to approximately 35% of expected hydrogen demand in 2050. This value corresponds to an LCOH of \$1.56. This suggests that a renewable hydrogen supply chain as proposed in this work is economically viable to operate.

An analysis of low-carbon hydrogen production methods is carried out, focusing on the production costs. From this comparison, it is found that the economic performance of the proposed supply chain in this work is comparable to alternative low-carbon hydrogen supply chains. It is estimated that the costs of hydrogen production using conventional production methods with the addition of CCS are between 1.98 - 2.79 $\$/kg_{H_2}$ for SMR and 1.88-2.74 $\$/kg_{H_2}$ for GC. Other work for producing hydrogen using electrolysis estimates a price of between 1.66 - 2.64 $\$/kg_{H_2}$. Although the results of this work indicate a low price compared to alternative methods of hydrogen production, most of the estimates used in the cost comparison fall within the estimated cost range provided by the sensitivity analysis.

The largest contributors to the cost of hydrogen production in this work are found to be power production

(50.4%), electrolysis (27.2%), and transport (19.7%).

However promising the results of this study may seem, it must be noted that many assumptions are made, both implicitly and explicitly, in setting up the model. Both technological and economic parameter assumptions are made for the case study. Moreover, assumptions about energy supply and demand are made based on historic data. These assumptions all influence the overall results of the model and therefore extend to the economic feasibility of the supply chain.

There are some factors that influence the performance of the supply chain that are not taken into account in this model. Further cost reductions could be achieved by implementing electricity storage between power generation and electrolysis, reducing the capacity of the electrolysis plant. Economies of scale are not taken into account in the model, although it is expected that beyond a certain scale of operations, no further cost reductions can be achieved by economies of scale.

Finally, there are some factors that may inhibit the feasibility of the supply chain under consideration. Firstly, transport costs for end-use distribution are not taken into account. As the cost contribution of transportation in the proposed supply chain is already over 25% of the total costs, this may impose a significant increase in overall costs. Secondly, system losses apart from the electrolyzer are not taken into account. Thirdly, the required land area for the PV plant is significant, at approximately 3.5% of the total land area of Morocco. It is questionable to assume that this land area is available in one location, as it would require the infrastructure necessary to build and maintain the solar plant. Finally, in terms of energy security, it may be advantageous to diversify the energy supply to the EU, rather than having 35% of energy imports come from a single supply chain.

The efforts of this work clearly indicate that a renewable hydrogen supply chain between Morocco and the EU could be technically and economically feasible, able to produce 780 TWh of hydrogen at $1.56\$/kg_{H_2}$. However, this work is an exploratory study of the topic, and it is expected that further research would be able to improve the system's performance. Further cost reductions are likely possible through improving the system design as well as further optimization of system operations.

Bibliography

1. Olson, C. & Lenzmann, F. The social and economic consequences of the fossil fuel supply chain. *MRS Energy & Sustainability* **3** (2016).
2. Gupta, J. A history of international climate change policy. *WIREs Climate Change* **1**, 636–653 (2010).
3. *Paris Agreement 2015*. https://treaties.un.org/pages/ViewDetails.aspx?src=TREATY&mtdsg_no=XXVII-7-d&chapter=27&clang=_en (2019).
4. European Commission. *The European Green Deal 2019*.
5. European Commission. *REPowerEU Plan 2022*.
6. Eurostat. *Energy Imports Dependency 2021*. https://ec.europa.eu/eurostat/databrowser/view/NRG_IND_ID__custom_938402/bookmark/table?lang=en,en&bookmarkId=f1ab4519-82df-4a89-a329-1b8d0a5925f7.
7. European Council. *Impact of Russia's invasion of Ukraine on the markets: EU response* Online. 2022. <https://www.consilium.europa.eu/en/policies/eu-response-ukraine-invasion/impact-of-russia-s-invasion-of-ukraine-on-the-markets-eu-response/>.
8. Van Wijk, A. & Wouters, F. in *Shaping an Inclusive Energy Transition* 91–119 (Springer International Publishing, 2021).
9. International Energy Agency. *World 2021*. <https://www.iea.org/world>.
10. Bhagwat, S. R. & Olczak, M. *Green Hydrogen: Bridging the Energy Transition in Africa and Europe* tech. rep. (Florence School of Regulation, 2020). <https://africa-eu-energy-partnership.org/publications/green-hydrogen-bridging-the-energy-transition-in-africa-europe/>.
11. Solargis. 2021. <https://solargis.com/maps-and-gis-data/download/africa>.
12. Global Wind Atlas. 2021. <https://globalwindatlas.info/>.
13. *Agenda 2063 : the Africa we want* ISBN: 9789295104235 (African Union Commission, Addis Ababa, 2015).
14. AbouSeada, N. & Hatem, T. M. Climate action: Prospects of green hydrogen in Africa. *Energy Reports* **8**, 3873–3890 (2022).
15. United Nations. Sustainable Development Goal 6: Synthesis Report on Water and Sanitation. https://d306pr3pise04h.cloudfront.net/docs/publications%2FSDG6_SR2018.pdf (2018).
16. Naik, P. K. Water crisis in Africa: myth or reality? *International Journal of Water Resources Development* **33**, 326–339. eprint: <https://doi.org/10.1080/07900627.2016.1188266>. <https://doi.org/10.1080/07900627.2016.1188266> (2017).

17. Chitonge, H. Urbanisation and the water challenge in Africa: Mapping out orders of water scarcity. *African Studies* **79**, 192–211. eprint: <https://doi.org/10.1080/00020184.2020.1793662>. <https://doi.org/10.1080/00020184.2020.1793662> (2020).
18. Li, L., Manier, H. & Manier, M.-A. Hydrogen supply chain network design: An optimization-oriented review. *Renewable and Sustainable Energy Reviews* **103**, 342–360 (2019).
19. Almansoori, A. & Shah, N. Design and operation of a future hydrogen supply chain: Multi-period model. *International Journal of Hydrogen Energy* **34**, 7883–7897 (2009).
20. Kim, J., Lee, Y. & Moon, I. Optimization of a hydrogen supply chain under demand uncertainty. *International Journal of Hydrogen Energy* **33**, 4715–4729 (2008).
21. INGASON, H., PALLINGOLFSSON, H. & JENSSON, P. Optimizing site selection for hydrogen production in Iceland. *International Journal of Hydrogen Energy* **33**, 3632–3643 (2008).
22. Almaraz, S. D.-L., Azzaro-Pantel, C., Montastruc, L. & Domenech, S. Hydrogen supply chain optimization for deployment scenarios in the Midi-Pyrénées region, France. *International Journal of Hydrogen Energy* **39**, 11831–11845 (2014).
23. Nunes, P., Oliveira, F., Hamacher, S. & Almansoori, A. Design of a hydrogen supply chain with uncertainty. *International Journal of Hydrogen Energy* **40**, 16408–16418 (2015).
24. Doodeman, R. *Costs competitive large-scale green hydrogen production in North-Africa in 2030*. □ MA thesis (TU Delft, 2022).
25. Roobeek, R. *Shipping Sunshine* MA thesis (TU Delft, 2020).
26. BALL, M., WIETSCHEL, M. & RENTZ, O. Integration of a hydrogen economy into the German energy system: an optimising modelling approach. *International Journal of Hydrogen Energy* **32**, 1355–1368 (2007).
27. Hajimiragha, A., Fowler, M. W. & Cañizares, C. A. Hydrogen economy transition in Ontario – Canada considering the electricity grid constraints. *International Journal of Hydrogen Energy* **34**, 5275–5293 (2009).
28. Sabio, N., Gadalla, M., Guillén-Gosálbez, G. & Jiménez, L. Strategic planning with risk control of hydrogen supply chains for vehicle use under uncertainty in operating costs: A case study of Spain. *International Journal of Hydrogen Energy* **35**, 6836–6852 (2010).
29. Woo, Y.-b., Cho, S., Kim, J. & Kim, B. S. Optimization-based approach for strategic design and operation of a biomass-to-hydrogen supply chain. *International Journal of Hydrogen Energy* **41**, 5405–5418 (2016).
30. Almansoori, A. & Betancourt-Torcat, A. Design of optimization model for a hydrogen supply chain under emission constraints - A case study of Germany. *Energy* **111**, 414–429 (2016).
31. Agnolucci, P., Akgul, O., McDowall, W. & Papageorgiou, L. G. The importance of economies of scale, transport costs and demand patterns in optimising hydrogen fuelling infrastructure: An exploration with SHIPMod (Spatial hydrogen infrastructure planning model). *International Journal of Hydrogen Energy* **38**, 11189–11201 (2013).
32. Almaraz, S. D.-L., Azzaro-Pantel, C., Montastruc, L. & Boix, M. Deployment of a hydrogen supply chain by multi-objective/multi-period optimisation at regional and national scales. *Chemical Engineering Research and Design* **104**, 11–31 (2015).

33. Bique, A. O. & Zondervan, E. An outlook towards hydrogen supply chain networks in 2050 — Design of novel fuel infrastructures in Germany. *Chemical Engineering Research and Design* **134**, 90–103 (2018).
34. Dayhim, M., Jafari, M. A. & Mazurek, M. Planning sustainable hydrogen supply chain infrastructure with uncertain demand. *International Journal of Hydrogen Energy* **39**, 6789–6801 (2014).
35. Cho, S., Woo, Y.-b., Kim, B. S. & Kim, J. Optimization-based planning of a biomass to hydrogen (B2H₂) system using dedicated energy crops and waste biomass. *Biomass and Bioenergy* **87**, 144–155 (2016).
36. HyUnder. *Project overview* online. 2015. <http://hyunder.eu/project-overview/>.
37. Robles, J. O., Almaraz, S. D.-L. & Azzaro-Pantel, C. in *Hydrogen Supply Chains* 37–79 (Elsevier, 2018).
38. Mallapragada, D. S., Gençer, E., Insinger, P., Keith, D. W. & O’Sullivan, F. M. Can Industrial-Scale Solar Hydrogen Supplied from Commodity Technologies Be Cost Competitive by 2030? *Cell Reports Physical Science* **1**, 100174 (2020).
39. Smale, C. *Inclusive carbon neutral pathways –Assessing the role of two renewable energy supply chains between Africa and the EU in greening their respective energy mix* MA thesis (TU Delft, 2022).
40. Khan, J. & Arsalan, M. H. Solar power technologies for sustainable electricity generation – A review. *Renewable and Sustainable Energy Reviews* **55**, 414–425 (2016).
41. Weller, B., Hemmerle, C., Jakubetz, S. & Unnewehr, S. *Detail Practice: Photovoltaics : Technology, Architecture, Installation* <http://ebookcentral.proquest.com/lib/delft/detail.action?docID=1075522> (Walter de Gruyter GmbH, Basel/Berlin/Boston, SWITZERLAND, 2010).
42. Sidi, P., Raden, N. & Hartanto, D. in *Solar Cells - Silicon Wafer-Based Technologies* (InTech, 2011).
43. Shah, A. in *Solar Cells and Modules* 33–72 (Springer International Publishing, 2020).
44. Bayod-Rújula, A. A. in *Solar Hydrogen Production* 237–295 (Elsevier, 2019).
45. Gao, F.-Y., Yu, P.-C. & Gao, M.-R. Seawater electrolysis technologies for green hydrogen production: challenges and opportunities. *Current Opinion in Chemical Engineering* **36**, 100827 (2022).
46. Ullah, I. & Rasul, M. Recent Developments in Solar Thermal Desalination Technologies: A Review. *Energies* **12**, 119 (2018).
47. Shatat, M. & Riffat, S. B. Water desalination technologies utilizing conventional and renewable energy sources. *International Journal of Low-Carbon Technologies* **9**, 1–19 (2012).
48. Soliman, M. N. *et al.* Energy consumption and environmental impact assessment of desalination plants and brine disposal strategies. *Process Safety and Environmental Protection* **147**, 589–608 (2021).
49. Curto, D., Franzitta, V. & Guercio, A. A Review of the Water Desalination Technologies. *Applied Sciences* **11**, 670 (2021).
50. Millet, P. in *Electrochemical Power Sources: Fundamentals, Systems, and Applications* 37–62 (Elsevier, 2022).

51. Stolten, D. *Hydrogen Production* ISBN: 3527333428. https://www.ebook.de/de/product/22845533/detlef_stolten_hydrogen_production.html (Wiley-VCH GmbH, 2015).
52. Sheffield, J. *et al.* A Study of Options for the Deployment of Large Fusion Power Plants. *Fusion Science and Technology* **40**, 1–36 (2001).
53. Millet, P. & Grigoriev, S. in *Renewable Hydrogen Technologies* (eds Gandía, L. M., Arzamendi, G. & Diéguez, P. M.) 19–41 (Elsevier, Amsterdam, 2013). ISBN: 978-0-444-56352-1. <https://www.sciencedirect.com/science/article/pii/B9780444563521000027>.
54. Thomassen, M. S., Reksten, A. H., Barnett, A. O., Khoza, T. & Ayers, K. in *Electrochemical Power Sources: Fundamentals, Systems, and Applications* 199–228 (Elsevier, 2022).
55. Brisse, A., Schefold, J. & Léon, A. in *Electrochemical Power Sources: Fundamentals, Systems, and Applications* 229–280 (Elsevier, 2022).
56. Óvári, M., Tarsoly, G., Németh, Z., Mihucz, V. G. & Zárny, G. Investigation of lanthanum-strontium-cobalt ferrites using laser ablation inductively coupled plasma-mass spectrometry. *Spectrochimica Acta Part B: Atomic Spectroscopy* **127**, 42–47 (2017).
57. Guo, Y., Li, G., Zhou, J. & Liu, Y. Comparison between hydrogen production by alkaline water electrolysis and hydrogen production by PEM electrolysis. *IOP Conference Series: Earth and Environmental Science* **371**, 042022 (2019).
58. Hu, K. *et al.* Comparative study of alkaline water electrolysis, proton exchange membrane water electrolysis and solid oxide electrolysis through multiphysics modeling. *Applied Energy* **312**, 118788 (2022).
59. Buttler, A. & Spliethoff, H. Current status of water electrolysis for energy storage, grid balancing and sector coupling via power-to-gas and power-to-liquids: A review. *Renewable and Sustainable Energy Reviews* **82**, 2440–2454 (2018).
60. Jacobsen, R. T., Leachman, J. W., Penoncello, S. G. & Lemmon, E. W. Current Status of Thermodynamic Properties of Hydrogen. *International Journal of Thermophysics* **28**, 758–772 (2007).
61. Godula-Jopek, A., Jehle, W. & Wellnitz, J. *Hydrogen Storage Technologies* 254 pp. https://www.ebook.de/de/product/21194005/agata_godula_jopek_walter_jehle_joerg_wellnitz_hydrogen_storage_technologies.html (Wiley-VCH Verlag GmbH Co. KGaA, July 2012).
62. Osman, A. I. *et al.* Hydrogen production, storage, utilisation and environmental impacts: a review. *Environmental Chemistry Letters* **20**, 153–188 (2021).
63. Bünger, U., Michalski, J., Crotagino, F. & Kruck, O. in *Compendium of Hydrogen Energy* 133–163 (Elsevier, 2016).
64. Tarkowski, R. Underground hydrogen storage: Characteristics and prospects. *Renewable and Sustainable Energy Reviews* **105**, 86–94 (2019).
65. Muhammed, N. S. *et al.* A review on underground hydrogen storage: Insight into geological sites, influencing factors and future outlook. *Energy Reports* **8**, 461–499 (2022).
66. Ozarslan, A. Large-scale hydrogen energy storage in salt caverns. *International Journal of Hydrogen Energy* **37**, 14265–14277 (2012).
67. Dopffel, N., Jansen, S. & Gerritse, J. Microbial side effects of underground hydrogen storage – Knowledge gaps, risks and opportunities for successful implementation. *International Journal of Hydrogen Energy* **46**, 8594–8606 (2021).

68. Schulze, O., Popp, T. & Kern, H. Development of damage and permeability in deforming rock salt. *Engineering Geology* **61**, 163–180 (2001).
69. Portarapillo, M. & Benedetto, A. D. Risk Assessment of the Large-Scale Hydrogen Storage in Salt Caverns. *Energies* **14**, 2856 (2021).
70. Copeland, T. E. & Wilson, J. F. *Financial Theory and Corporate Policy* (Addison-Wesley Publishing Company, 1988).
71. Fuel Cells and Hydrogen 2 Joint Undertaking. *Hydrogen roadmap Europe :a sustainable pathway for the European energy transition*. (Publications Office, 2016).
72. eurostat. *Supply, transformation and consumption of electricity - monthly data 2022*. https://ec.europa.eu/eurostat/databrowser/view/NRG_CB_EM__custom_2482476/default/table.
73. NASA POWER. *POWER | Data Access Viewer 2022*. <https://power.larc.nasa.gov/data-access-viewer/>.
74. IRENA. *Renewable Power Generation Costs in 2019* tech. rep. (International Renewable Energy Agency, Abu Dhabi, 2020).
75. Pregger, T., Simon, S., Naegler, T. & Teske, S. in *Achieving the Paris Climate Agreement Goals* 93–130 (Springer International Publishing, 2019).
76. GL, D. *Energy transition outlook 2019: A global and regional forecast to 2050: Technical report* tech. rep. (2019). <https://eto.dnvg1.com/2019>.
77. Brändle, G., Schönfisch, M. & Schulte, S. Estimating long-term global supply costs for low-carbon hydrogen. *Applied Energy* **302**, 117481 (2021).
78. IRENA. *GREEN HYDROGEN COST REDUCTION* tech. rep. (2020).
79. Roos, T. H. The cost of production and storage of renewable hydrogen in South Africa and transport to Japan and EU up to 2050 under different scenarios. *International Journal of Hydrogen Energy* **46**, 35814–35830 (2021).
80. Caldera, U. & Breyer, C. Learning Curve for Seawater Reverse Osmosis Desalination Plants: Capital Cost Trend of the Past, Present, and Future. *Water Resources Research* **53**, 10523–10538 (2017).
81. Lampert, D. *et al. Development of a Life Cycle Inventory of Water Consumption Associated with the Production of Transportation Fuels* tech. rep. (Argonne National Laboratory, 2015).
82. Rhodes, C. *Electricity Transmission* July 2020. <https://www.xylenepower.com/Transmission%20Concepts.htm>.
83. MISO Energy. *Transmission Cost Estimation Guide* tech. rep. (2019). https://cdn.misoenergy.org/20190212%20PSC%20Item%2005a%20Transmission%20Cost%20Estimation%20Guide%20for%20MTEP%202019_for%20review317692.pdf.
84. Juez-Larré, J., van Gessel, S., Dalman, R., Remmelts, G. & Groenenberg, R. Assessment of underground energy storage potential to support the energy transition in the Netherlands. *First Break* **37**, 57–66 (2019).
85. Michalski, J. *et al.* Hydrogen generation by electrolysis and storage in salt caverns: Potentials, economics and systems aspects with regard to the German energy transition. *International Journal of Hydrogen Energy* **42**, 13427–13443 (May 2017).

86. Eradus, D. *The Techno-Economic Feasibility Of Green Hydrogen Storage in Salt Caverns in The Dutch North Sea* MA thesis (TU Delft, Jan. 2022).
87. MERCOM. *With 2,245 MW of Commissioned Solar Projects, World's Largest Solar Park is Now at Bhadla | Mercom India 2020*. <https://mercomindia.com/world-largest-solar-park-bhadla/>.
88. Ong, S., Campbell, C., Denholm, P., Margolis, R. & Heath, G. *Land-Use Requirements for Solar Power Plants in the United States* tech. rep. (2013).
89. IEA. *The Future of Hydrogen* Online. 2019. <https://www.iea.org/reports/the-future-of-hydrogen>.
90. Water technology. *Sorek desalination plant 2022*. <https://www.water-technology.net/projects/sorek-desalination-plant/#:~:text=The%20Sorek%20desalination%20is%20the,south%20of%20Tel%20Aviv,%20Israel..>
91. CSIRO. *National Hydrogen Roadmap* tech. rep. (CSIRO, 2018).
92. NREL. *Electrolysis' Potential Value for Supporting the Electrical Grid* in (2019).
93. IRENA. *HYDROGEN: A RENEWABLE ENERGY PERSPECTIVE* tech. rep. (IRENA, 2019).
94. Bloomberg NEF. *Hydrogen Economy Outlook Key messages 2020*.
95. Salkuyeh, Y. K., Saville, B. A. & MacLean, H. L. Techno-economic analysis and life cycle assessment of hydrogen production from natural gas using current and emerging technologies. *International Journal of Hydrogen Energy* **42**, 18894–18909 (2017).
96. International Energy Agency Greenhouse Gas (IEAGHG) RD Programme. *2017-TR3 REFERENCE DATA SUPPORTING LITERATURE REVIEWS FOR SMR BASED HYDROGEN PRODUCTION WITH CCS 2017*.
97. CE Delft. *Feasibility study into blue hydrogen* tech. rep. (2018).
98. International Energy Agency Greenhouse Gas (IEAGHG) RD Programme. *Capture at coal based power and hydrogen plants 2014*.
99. IEA. *CCUS in Clean Energy Transitions – Analysis* tech. rep. (2020).
100. entsog. *TRANSMISSION CAPACITY AND SYSTEM DEVELOPMENT MAPS* Nov. 2021. <https://www.entsog.eu/maps#transmission-capacity-map-2021>.